Investigating bacteria-bacteriophage interactions underlying inflammatory bowel disease

Ji Hyun Yong

Department of Medical Science

The Graduate School, Yonsei University

Investigating bacteria-bacteriophage interactions underlying inflammatory bowel disease

Directed by Professor Sang Sun Yoon

The Doctoral Dissertation
submitted to the Department of Medical Science,
the Graduate School of Yonsei University
in partial fulfillment of the requirements for the
degree of Doctor of Philosophy in Medical Science

Ji Hyun Yong

June 2023

This certifies that the Doctoral Dissertation of Ji Hyun Yong is approved.

Thesis Supervisor : Sang Sun Yoon

Thesis Committee Member#1 : Jun-Young Seo

Thesis Committee Member#2 : Jae Hee Cheon

Thesis Committee Member#3: Minsik Kim

Thesis Committee Member#4: Kihyuck Kwak

The Graduate School
Yonsei University

June 2023

ACKNOWLEDGEMENTS

지난 5년 동안 애정 어린 관심과 지원으로 제 학위과정을 지도해 주신 윤상선 교수님께 감사드립니다. 교수님께서 제공해 주신 품 안에서 연구자로서 크게 성장할 수 있었고, 그 과정에서 좋은 인연들을 많이 만들 수 있었습니다. 감사한 마음 잊지 않고, 받은 만큼 베풀 수 있는 사람이 되도록 하겠습니다. 그리고 바쁘신 와중에도 제 졸업과정에서 진심 어린 자문을 해 주신 서준영 교수님, 천재희 교수님, 김민식 교수님, 곽기혁 교수님께 감사드립니다.

실험실 식구들에게도 모두 감사드립니다. 장내 미생물이 생경했던 저에게 많은 가르침을 주시고 늘 배움에 대한 열정이 존경스러운 윤미영 박사님, 실험실의 어른으로 늘 따뜻하게 대해주시고 cloning 실험에 많은 조언을 주셨던 이강무 박사님, 늘 한결같은 모습과 조용하지만 뜨거운 열정으로 좋은 연구자의 본보기가 되어 주신 김지은 박사님께 감사드립니다.

2018년 6월에 처음 들어와 미생물 실험실이 낯선 저에게, 누구보다 먼저 가까이서 많은 걸 아낌없이 알려주고, 수많은 시간을 BL3 와 SPF 에서 동고동락했던 유진선 박사님께 감사드립니다. 또, 실험실의 큰형/오빠로 솔선수범해주신 김광희 박사님, 늘 웃는 얼굴로 즐거운 시간들을 함께했던 이유진 박사님께도 감사드립니다. 늘 새로운 생각과 호기심으로 늦은 시간까지 자리를 지키는 Mohammed 선생님도 고마웠고 좋은 결과로 학위 마무리하시리라 믿습니다.

지금은 실험실을 떠나셨지만, 각자의 자리에서 열심히 지내고 계실 민경배 박사님, 김태강 선생님, 김동근 선생님, 동기 다현이, 최리나 선생님 그리고 김화영 박사님도 모두 그립고 고마웠습니다. 김시형 박사님과 정욱진 선생님도 짧은 시간이지만 같은 분단에서 함께 할 수 있어서 좋았습니다. 또, 학위과정의 많은 시간을 함께 하고 신촌 근방의 맛집들을 알려주신 정찬민 선생님, 바쁜 스케줄에도 늘 에너자이저셨던 슈퍼우먼 박소원 선생님, 그리고 마음이 힘들 때 의지가 되어준 언니같은 윤이 선생님도 많이 고마웠고 그리울 것 같습니다.

제가 많이 부족한 선배임에도 좋게 봐줬던 후배들도 참 고마웠습니다. 본인의 호기심을 좇아 새로운 도전을 하고 있는 채영이, 늘 에너지 넘치는 모습으로 맛있는 음식을 해주던 준범이, 배려심과 센스가 넘치는 인싸 경진이, 아침 일찍 마주치면 조용히 초코우유를 챙겨주던 윤지, 늘 웃는 모습이지만 속은 단단한 쿼카 지원이, 밤낮 구분없이 열심인 꿈나무 성혁이와 솔직하고 당당함이 멋진 현아 모두 고마웠고, 앞으로도 많은 성장과 즐거운 일들이 가득하기를 기원합니다.

I would also like to thank everyone in the Camilli lab for the warm and welcoming environment they provided during my time at Tufts. Thank you, Andy, for letting me share a part of your bay and giving me the courage and inspiration I needed to finish my thesis project. Thank you, Liz, Kyle, Yishak, Dave and Andrea for all the discussions and fun we had. I miss you all lots and wish you best of luck with all your endeavours.

마지막으로, 제가 박사학위를 따기까지, 지난 30여년간 많은 노력과 희생으로 저를 하나의 인간으로 성장시켜 주신 부모님 용동은, 김문숙님께 깊이 감사드립니다. 어떤 감사의 말도 부족하겠지만, 행복하고 건강하게 잘 사는 모습으로 보답하도록 하겠습니다. 동생 정호도, 그리고 은지도, 제가 학위를 따는데 많은 힘이 되어주어 고맙고 늘 응원합니다.

그리고, 제 남편 황원태 박사에게도 감사를 전합니다. 정보학을 궁금해하던 후배였던 저를, 본인이 닦은 길로 아낌없이 인도해줬었는데, 이제는 결혼이란 인생의 챕터를 함께 써 나가고 있네요. 부족한 모습 또한 아껴주고 함께 노력해줘서 고맙습니다. 앞으로도 잘해봅시다.

모두들 상황과 무관하게 즐거운 날들이 되시길 바랍니다.
감사합니다.

2023년 6월 용지현 올림

<TABLE OF CONTENTS>

LIST OF FIGURES

LIST OF TABLES

ABSTRACT

Investigating bacteria-bacteriophage interactions underlying inflammatory bowel disease

Ji Hyun Yong

Department of Medical Science
The Graduate School, Yonsei University

(Directed by Professor Sang Sun Yoon)

Two murine gut commensal *Escherichia coli* strains and their phages were used as a model system in investigating bacteriophage-*E. coli* interactions in inflammatory bowel disease (IBD)-like environment. To this end, two novel bacteriophages, ϕt*Ec* and ϕat*Ec*, targeting two strains of *E. coli* were isolated from sewage and characterized. Through genome sequencing, the two phages ϕt*Ec* and ϕat*Ec* were predicted to replicate using distinct Proteobacterial hosts, and each belong to families *Drexlerviridae* and *Straboviridae*, respectively. Interestingly, under the presence of reactive oxygen species (ROS) stress, *E. coli* were more tolerant of phage-mediated lysis. Transposon sequencing revealed the lists of genes that mediate sensitivity or resistance to phage under ROS condition. Genes that conferred increased tolerance to phage killing were involved in multidrug efflux pump (*mdtE*), colonic acid capsule biosynthesis (*manC*), toxin (*hokA*), prophage excisionase (*xisR*), and stress response (*yciH*, *yhbO*).

Considering the prevalence of *E. coli* in IBD and the co-existence of phages that can target these bacteria in the gut, we propose that the high level of ROS in IBD may be inducing a phage tolerant phenotype in gut commensal *E. coli*, which in turn may contribute to the uncontrolled proliferation of *E. coli* in IBD that is widely reported.

Key words : *Escherichia coli*, gut commensal bacteria, inflammatory bowel disease, bacteriophage, reactive oxygen species

Investigating bacteria-bacteriophage interactions underlying inflammatory bowel disease

Ji Hyun Yong

Department of Medical Science
The Graduate School, Yonsei University

(Directed by Professor Sang Sun Yoon)

I. INTRODUCTION

1. What are bacteriophages?

Bacteriophages, also known as phages, are viruses that infect and replicate within bacteria. They are the most abundant biological entities on Earth and can be found in virtually every environment, from soil and water to the human gut[1-6]. Bacteriophages are incredibly diverse in terms of their size, shape, and genetic makeup. They can range from 20 to 200 nanometers in size[7, 8] and can have either DNA or RNA as their genetic material. Bacteriophages have a complex structure, consisting of a protein coat or "capsid" that encloses their genetic material. Some phages have an additional layer called an "envelope" that surrounds the capsid[9, 10]. The envelope is made up of lipids and proteins and is derived from the host bacterial cell membrane during the viral replication cycle.

The replication cycle of bacteriophages involves several steps. In case of virulent phages, first, the phage attaches to a specific receptor on the surface of

the host bacterium. This recognition step is crucial for determining which bacteria a particular phage can infect. Once attached, the phage injects its genetic material into the host cell, where it hijacks the bacterial machinery to produce new viral particles. Eventually, the newly formed phages are released from the host cell through lysis[11]. The released phages can then go on to infect other bacterial cells and continue the cycle of replication. In the case of temperate phages, they carry out a lysogenic life cycle, wherein the initial attachment and injection of genetic material occur in a similar fashion as those of virulent phages. However, rather than the injected genetic material being used for synthesis of new viral particles, it gets integrated into the host bacterial genome. Often, introduction of a stressor, for example nutrient starvation condition, induces the temperate phage to enter lytic cycle, while spontaneous lytic cycle can occur in the absence of an obvious stressor[12]. Hence, the fate of the temperate phage thus becomes intertwined with that of the host. Lysogenic lifestyle constrains the phage replication to the rate of the host cell's binary fission, while it allows the lysogenized prophage the opportunity to alter the host cell physiology through regulation of its gene expression[13] or by introducing novel functions through process called 'lysogenic conversion'[14]. In addition to these two lifestyles, pseudolysogeny may occur, where the injected phage genetic material does not integrate into the host genome but exists as an episome within the host without actively producing new viral particles[15].

Hence, given the innate ability of the bacteriophages to affect bacterial

populations, bacteriophages have long been studied as potential therapeutic agents for bacterial infections, particularly those that are resistant to antibiotics. Phages have a number of advantages over traditional antibiotics, including their ability to specifically target certain bacterial strains and their ability to evolve alongside their host bacteria, making it more difficult for bacteria to develop resistance[16]. Furthermore, several studies have reported a synergistic effect of antibiotics-phage combination treatment[17-19]. However, more research is needed to fully understand the potential of phage therapy and to develop safe and effective treatments.

2. Role of commensal bacteria and endogenous phages on host health

In the human gut, commensal bacteria perform various functions that facilitate normal physiology of the host. For example, commensal strains of *Roseburia hominis* and *Faecalibacterium prausnitzii* have been shown to produce metabolites such as butyrate that promote strengthening of the intestinal epithelial barrier[20], and other commensal bacteria such as *Eggerthella lenta* have been shown to convert the host-produced primary bile acid into secondary bile acid products that modulate the host immune response[21]. More recently, bacteriophages, or phages, have received renewed attention as an additional prominent component of the gut microbiota. Recent discoveries of the phages' co-colonization of the human gastrointestinal tract with the commensal bacteria

have led to investigations of how they might influence the bacterial population and furthermore host health[22-24]. For instance, administration of bacteriophages into the murine intestine colonized with a consortium of bacteria was shown to be effective at altering the bacterial composition[25], and multiple reports of altered gut phage compositions in inflammatory bowel disease (IBD) gut in comparison to normal intestine have been published[26, 27].

In IBD, a condition where there is a significant inflammation of the gut, dramatic expansion of the gut *Escherichia coli* population has been reported[28-30]. One of the key modulators of bacterial population size in the gut ecosystem is bacteriophages[25, 31, 32]. Thus, even though *E. coli* is better adapted and outcompetes other more strictly anaerobic gut commensal species when the oxygen potential increases as in IBD[33], it remains mysterious why the endogenous coliphage population is no longer able to limit the *E. coli* proliferation. Moreover, in no other microbiomes, as significant and unanimously reported as the Enterobacteriaceae expansion in IBD has been observed, suggesting that the IBD environment provides an important feature that facilitates such characteristic expansion. Since high oxidative stress is one of the defining characteristics of the IBD gut environment[34, 35] and simultaneously a major factor that supports the proliferation of *Enterobacteriaceae*[36-38], I hypothesized that ROS may be affecting change in *E. coli* such that they better resist killing by endogenous phages.

In order to study how gut commensal *E. coli* interact with phages in IBD-like

condition, we selected two gut commensal *E. coli* strains, t*Ec* and at*Ec*, isolated from antibiotic-treated mouse intestine in a previous study[39]. Antibiotic-treated gut environment is similar to that of IBD gut environment, in that in both are high levels of reactive oxygen species. This high ROS level is one of the main characteristics that distinguish the inflammatory bowel, and therefore a significant environmental stress for the bacteria that reside in the gut[35, 40]. Thus, as a model system of bacteriophage-*E. coli* interactions in IBD, we decided to use the two *E. coli* strains isolated from ROS-high intestine and their phages.

II. MATERIALS AND METHODS

1. Single phage isolation

Phages were isolated from a sample of wastewater collected at Yonsei university hospital by polyethylene glycol (PEG) precipitation method. Briefly, NaCl was added to the wastewater sample to 1M, and stored at 4 °C overnight. Subsequently, the sample was centrifuged at 13000 rpm for 10 min, and the supernatant was put through a 0.45 μm filter (Sartorius). PEG-8000 (10%, Merck, Boston, USA) was added to the filtered supernatant, and the suspension was stored at 4 °C overnight. Then, the stored suspension was centrifuged at 15000 rpm for 30 min. Resulting pellet was then resuspended in 2 mL of saline magnesium sulfate (SM) buffer (100 mM NaCl, 8 mM $MgSO_4 \cdot 7H_2O$, 50 mM

Tris-Cl). For enrichment of specific host-killing phages, 1 mL of the crude phage suspension was added to 40 mL of host bacterial culture and this mixture was incubated at 37 °C overnight with shaking at 230 rpm. Mixture of phage and bacteria was then centrifuged at 8000 rpm for 20 min, the supernatant was filtered using 0.22 μm filter, and PEG-8000 was added prior to overnight storage at 4 °C. Finally, the solution was centrifuged at 15000 rpm for 1 h, and the pellet was resuspended in 2 mL of SM buffer.

2. Phage genome extraction and whole genome sequencing

Phage genomic DNA was isolated from high-titer phage stocks (~10^9 PFU/mL) using Norgen Biotek phage DNA isolation kit (Cat. 46850, Canada). For whole genome sequencing of the phage DNA, sequencing library was prepared using Illumina DNA prep kit and indexes set (Cat. 20018704, 20027213; San Diego, CA, USA). Prepared sequencing libraries were sequenced using Illumina MiniSeq sequencer and the corresponding mid-output reagent kit (FC-420-1004; San Diego, CA, USA). Resulting sequence data was trimmed and quality controlled using Cutadapt[41]. Processed reads were then *de novo* assembled using SPADEs[42]. Assembled genomes were annotated using Prokka[43] and Phaster[44]. Further analysis and visualization were performed using CLC Genomic Workbench 20.0 (Qiagen, Aarhus, Denmark) and Proksee[45].

3. Phage killing experiments in reactive oxygen species (ROS)

Overnight cultures of host *E. coli* strains in Luria-Bertani miller (LB) broth were back diluted to OD_{600} 0.1 in fresh LB media supplemented with appropriate volumes of hydrogen peroxide (Sigma Aldrich; H1009-100ML). Phages were simultaneously added to the culture to multiplicity of infection of 0.1. The E.coli-phage mixture was then incubated at 37 °C with shaking at 230 rpm for 3 h. Subsequently, number of viable cells in the cultures were measured by serial dilution of the cultures and spotting on LB plates.

4. Random transposon mutagenesis

Transposon-containing plasmid pBTK30 with a gentamicin resistance marker was transformed into t*Ec* and at*Ec* by conjugation with *E. coli* χ7213. The transposon mutant libraries of t*Ec* and at*Ec* were cultured in 100 mL of LB media containing the corresponding phages at MOI of 1, at 37 °C overnight with shaking at 230 rpm. Overnight cultures were inoculated into 100 mL of fresh media containing phages and cultured as previously. After thus passaging the libraries under phage pressure, aliquots of the surviving cultures were plated onto LB plates. Dozen individual colonies of each t*Ec* and at*Ec* mutants that formed on the LB plates were isolated and the region into which the transposon had inserted, in each colony was identified by sequencing.

5. Pre-treatment of phage with ROS

~10^9 PFU of ϕt*Ec* and ϕat*Ec* were mixed with appropriate volumes of H_2O_2 in

LB media at 37 °C with shaking at 230 rpm for 1.5 h. Subsequently, catalase from bovine liver was added to solution at 100 U/mL (C9322, Merck, Boston, USA) and incubated at 37 °C for 30 min. Host bacterial cells were then added to the phage solution and incubated at 37 °C for 1.5 h with shaking at 230 rpm. Viable cell counts were performed on LB plates.

6. Sequential treatment of ROS and phage

Overnight cultures of t*Ec* (n=3) were back diluted to OD_{600} 0.1 in fresh LB media supplemented with appropriate concentrations of H_2O_2, and incubated for 2 h at 37 °C with shaking at 230 rpm. H_2O_2 pre-treated cells were collected and resuspended in fresh LB media. Phages were subsequently added at MOI 0.1 and viable cell counts were performed 2 h post-infection.

7. Transposon sequencing (Tn-seq) library construction

Overnight cultures of t*Ec* (n=3) were back diluted to OD_{600} 0.1 in fresh LB media supplemented with appropriate concentrations of H_2O_2, and incubated for 2 h at 37 °C with shaking at 230 rpm. H_2O_2 pre-treated cells were collected and resuspended in fresh LB media. Phages were subsequently added at MOI 0.1 and viable cell counts were performed 2 h post-infection.

8. Transposon sequencing (Tn-seq) passage

For passage under different stress conditions, a single aliquot of the t*Ec*/mTn10

was used for each replicate (n=2). Thawed library cells were diluted to OD_{600} 0.1, and 1 mL was inoculated into 300 mL LB broth. This culture was incubated overnight at 37 °C with shaking at 230 rpm. Next morning, 1 mL of the overnight cultures were taken to prepare gDNA of the input library using Qiagen Blood & Tissue kit. Overnight cultures were back diluted to OD_{600} 0.2 in fresh 100 mL of LB broth, containing different concentrations of H_2O_2 and/or phage (MOI = 0.1) as appropriate. Under different stress conditions, cultures were incubated for 3 h at 37 °C with shaking at 230 rpm. Finally, gDNA was extracted from the surviving cells in each output culture. Prior to sequencing the transposon insertion junctions, genomic DNA were prepared by HTML-PCR following the protocol previously described[46].

9. Bioinformatic analysis of Tn-seq data

Tn-seq data was processed as described previously[47]. Briefly, raw reads generated by sequencing the HTML-PCR products using Illumina Miseq were quality-filtered and adapter trimmed using CLC Genomics Workbench software. Processed reads were then aligned to the reference t*Ec* genome, and the output mapping files were used as input for Hopcount data analysis[48]. Using the Hopcount script and the annotated t*Ec* genome, frequency of each insertion mutant and thus dvalgenome (fitness) values of each gene under each stress condition were calculated. Candidates passing the statistical cutoff were selected.

10. Lambda Red recombineering for deletion mutant generation

Lambda red system-harbouring pKD46 was transformed into t*Ec* cells by electroporation. Successful transformants were selected on LB ampicillin (100 μg/ml) plates. Electrocompetent t*Ec*/pKD46 cells were made and used for downstream transformation of the DNA fragment. First, 50 bp regions flanking a candidate gene to be deleted were added to either end of a spectinomycin resistance cassette by PCR amplification. Purified PCR product was then mixed with electrocompetent t*Ec*/pKD46 cells and transformed via electroporation at 2.5 kV. Successful deletion mutants would gain spectinomycin resistance, and thus we selected the deletion mutants using LB plates supplemented with spectinomycin (100 μg/ml).

11. Mutant competition assay

In-frame deletion mutants were co-cultured in LB broth with wild type t*Ec* under same conditions as Tn-seq. At the end of 3 hours, cultures were serially diluted and 100 μl of each were spread on LB agar supplemented with 20 mg/ml X-gal and 100 mM IPTG, using sterile glass beads. After incubation at 37 °C overnight, numbers of each blue and white colonies were counted and used to calculate competitive indices for each strain.

12. Measurement of gene expression by real-time PCR

Overnight cultures of tEc (n=6) grown for 16 hours at 37 °C with shaking at 230

rpm were backdiluted to OD_{600} 0.1. When OD_{600} of the cultures reached 0.4, H_2O_2 was added to experimental group cultures to final concentration of 2 mM. After incubation at 37 °C with shaking at 230 rpm for 30 minutes, 1 mL of each culture was collected for subsequent RNA purification. Using Qiagen RNeasy Mini kit (Cat. 74104, Qiagen, Aarhus, Denmark), total RNA from cells were collected following the manufacturer's protocol. For quantitative PCR (qPCR), cDNA was synthesized from 1 μg of total RNA using random hexamer primers and SuperScript reverse transcriptase II (Invitrogen, Waltham, MA, USA). qPCR was performed using PowerUP SYBR Green Master Mix (Applied Biosystems, Waltham, MA, USA), and QuantStudio 3 Real-time PCR system (Applied Biosystems, Waltham, MA, USA). All data were collected using QuantStudio Design and Analysis software (v1.5.1, Applied Biosystems, Waltham, MA, USA) and normalized to universal 16S RNA and gene expression values were obtained using the ΔΔ-Ct method.

III. RESULTS

1. Isolation and characterization of coliphages

In order to investigate how gut commensal *Escherichia coli* strains interact with phages, we isolated phages from wastewater collected at Severance hospital, in Seoul, South Korea, following the protocol described in Material and Methods (Fig 1A). Single phages that form clear plaques on lawns of bacteria were purified and each phage was shown to target only t*Ec* or at*Ec* and not able to target the other bacterial strain (Fig 1B). Each of these phages are hereonafter referred to as ϕt*Ec* and ϕat*Ec*. When each phage-bacteria pairs were mixed at various multiplicity of infection (MOI), phages exhibited killing activity proportional to the MOI. At the lowest MOI of 0.0001, lysis of t*Ec* and at*Ec* occurred once OD_{600} reached approximately 0.5 and 0.6, respectively. At the highest MOI of 10, lysis of t*Ec* and at*Ec* occurred at OD_{600} of approximately 0.2 for both strains (Fig 2). Notably, t*Ec* infected with phage at MOI of 1 and 10 both exhibited emergence of phage resistance bacteria within 6 hours.

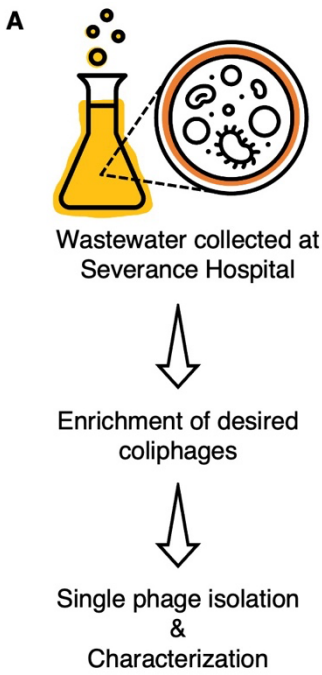

B

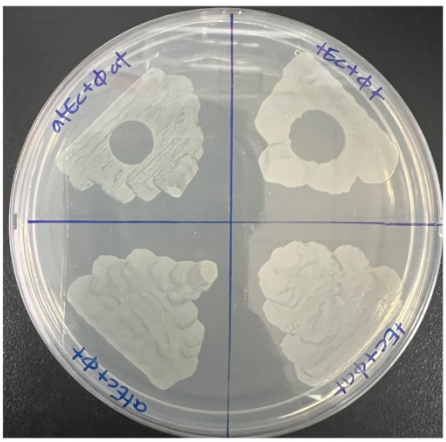

	t*Ec*	at*Ec*
ϕt*Ec*	**Lysis**	No lysis
ϕat*Ec*	No lysis	**Lysis**

Figure 1 Isolation and characterization of *E. coli*-targeting phages. (A) Wastewater sample collected at Severance hospital was enriched with host bacterial strains and single phages able to form clear plaques on t*Ec* and at*Ec* were isolated and purified. (B) Spot lysis test of the purified phage stocks revealed each phage can target either one of t*Ec* or at*Ec* but not both.

Table 1. Bacterial and phage strains, and plasmids used in this study

Strains/Plasmids	Description	Source
E. coli strains		
t*Ec*	Isolate from mouse intestine. Parental (wild-type) strain for gene deletion, wherein the target gene was replaced by spectinomycin adenyltransferase cassette derived from pDL1098.	[39]
at*Ec*	Isolate from mouse intestine.	[39]
DH5$_{\alpha}$ λpir	General cloning strain.	Lab Collection
Coliphages		
ϕt*Ec*	Phage isolated from sewage collected at a tertiary university hospital, targeting t*Ec*.	This study
ϕat*Ec*	Phage isolated from sewage collected at a tertiary university hospital, targeting at*Ec*.	This study
Plasmids		
pKD46	Lambda red recombineering plasmid inducible with arabinose, replicates at < 30°C; ampicillin resistant.	Lab Collection
pCVD442	Suicide vector used for deletion of *hokA* and *xisR;* ampicillin and gentamicin resistant.	Lab Collection
pDL1098	Transposition vector carrying mTn10 for Tn-seq, replicates at < 30°C; chloramphenicol and spectinomycin resistant.	[47]
pDL1086	Transposition vector carrying mTn10 for Tn-seq, replicates at < 30°C; chloramphenicol and ampicillin resistant.	[47]

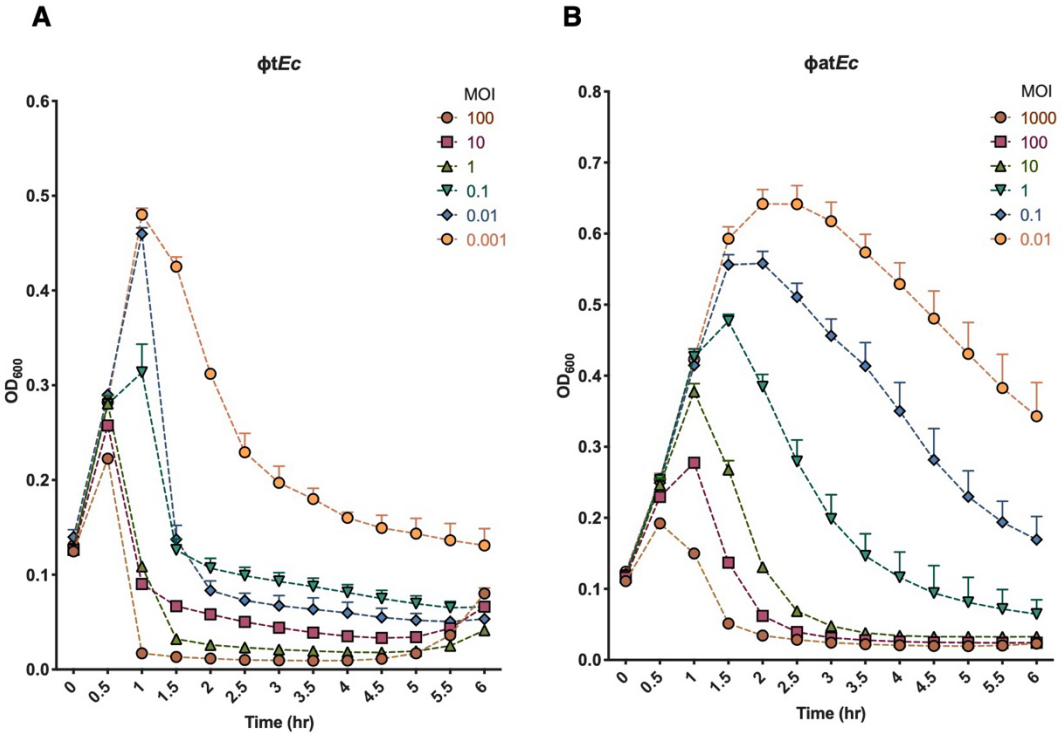

Figure 2 Lysis curves. Lysis curves of each pair (A) t*Ec*-ϕt*Ec* and (B) at*Ec*-ϕat*Ec* were measured by OD_{600}. Higher MOIs corresponded with increased lytic efficiency.

Additionally, since one of the key characteristics of bacteriophages is the specific range of hosts they can target, we characterized the host range of the two phages, using a panel of 65 clinical *E. coli* isolates for infection with each phage. Bacterial strains that the phage could use to replicate and form clear plaques by lysing the host cells were included in the phage's host range. ϕt*Ec* was able to replicate on 12 strains, whereas ϕa*Ec* was able to use 5 strains as host (Fig 3). Interestingly, the two phages shared only one host out of the 65 strains tested, indicating their high specificity for host. Moreover, this narrow overlap in host ranges was reflected in their largely variable genomic contents.

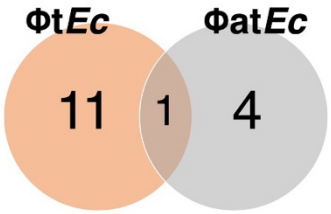

Clinical isolate		ΦtEc	ΦatEc	Clinical isolate		ΦtEc	ΦatEc	Clinical isolate		ΦtEc	ΦatEc
1	U4314	■		26	601			51	U816		
2	B4482			27	B11762			52	U973		
3	R434			28	P567			53	U1287		
4	P610			29	C750			54	U480		
5	U4093			30	B9259			55	U1142		
6	C644			31	N486			56	U1460	■	
7	B5019			32	MS1341			57	U1740		
8	P385			33	N515			58	U1795		
9	B7608			34	N407			59	U2093		■
10	U3929	■		35	N442			60	U1838	■	
11	T164			36	N459			61	U2267		
12	U4257			37	N47			62	U2245		
13	B11671			38	U4711			63	U2404		
14	N27			39	N477			64	U2448		
15	P406			40	MS1043			65	U208	■	
16	N8			41	N467						
17	N32			42	N243						
18	U3948			43	N337						
19	N86		■	44	MS1350	■					
20	C611			45	B14276						
21	N413	■		46	P846						
22	N678	■		47	N112	■					
23	U5634			48	N218		■				
24	N595	■		49	B13141						
25	N759	■	■	50	N231						

■ Lysis
No lysis

Figure 3 Host range of ϕt*Ec* and ϕat*Ec*. Host ranges of ϕt*Ec* and ϕat*Ec* were investigated using a panel of 65 clinical isolate *E. coli* strains. Only one out of 65 host bacterial strains was shared by the two phages.

Phage genomes were extracted and sequenced from the single phage stocks, and bioinformatically analysed. Genome of the ϕat*Ec* was much larger than that of ϕt*Ec,* where each was 39kbp (Fig 4) and 167kbp (Fig 5) long. Reflective of "viral dark matter", or our currently limited knowledge in phage proteins, most of the predicted coding sequences were not annotated by Prokka or Phigaro, tools used to annotate the phage genomes. The two phage genomes were used to generate a predicted proteome, and they were compared to an online database of 4913 prokaryotic dsDNA viruses, to estimate their hosts and viral family (Fig 6). ϕt*Ec* and ϕat*Ec* were both predicted to target Proteobacterial hosts, to which *E. coli* belongs, and each belong to families *Drexlerviridae* and *Straboviridae*, respectively.

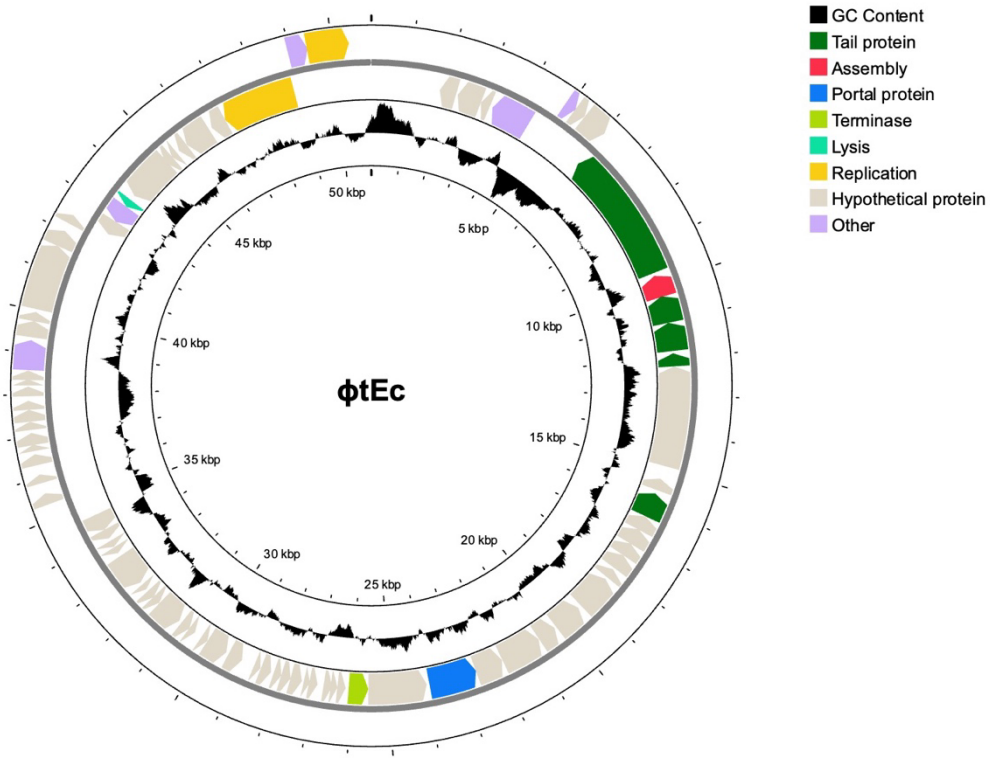

Genome Size (bp)	Number of CDS	G + C content
39,593	83	45.07%

Figure 4 ϕt*Ec* genome map. Features of ϕt*Ec* genome and map created using whole genome sequencing data and Proksee.

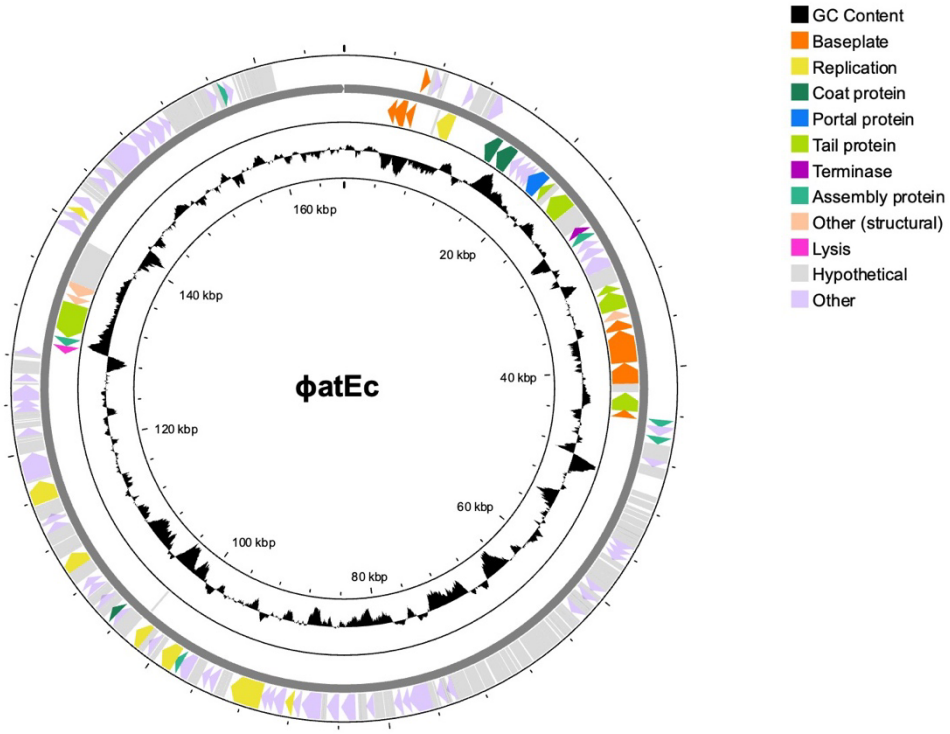

Genome Size (bp)	Number of CDS	G + C content
167,107	261	35.44%

Figure 5 ϕat*Ec* genome map. Features of ϕat*Ec* genome and map created using whole genome sequencing data and Proksee.

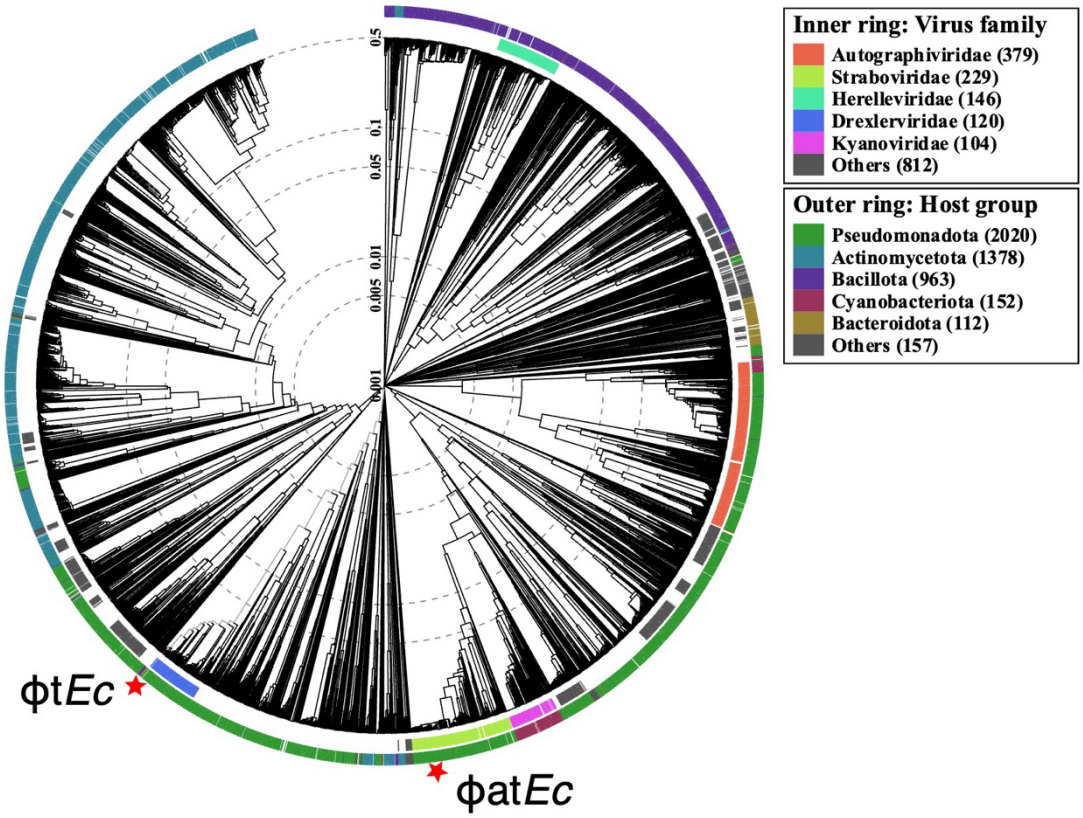

Figure 6 Proteomic tree of ϕt*Ec* and ϕat*Ec*. Proteomic tree was drawn based on the translated genomes of ϕt*Ec* and ϕat*Ec* phages in relation to 4913 prokaryotic virus genomes publicly available. Inner ring depicts the viral family the phage is predicted to belong to, and the outer ring indicates the most likely host group the phage may use as host. Red stars indicate where the two phages are in relation to each other.

2. Identification of putative host receptor proteins

Phages are known to use specific receptors on host bacterial cell to establish adsorption and initiate infection. This specific selection of host receptor proteins may attribute to the specific nature of host selection among phages. To identify which host receptors each phage uses to infect their hosts, we performed random transposon mutagenesis of the two host *E. coli* strains. Bacterial mutants that exhibited resistance to the corresponding phage were isolated and the gene disrupted by transposon insertion was identified by sequencing (Fig 7A). Based on sequencing results, phages ϕt*Ec* and ϕat*Ec* were shown to use TonB-dependent vitamin B12 receptor BtuB and outer membrane protein C as putative host receptors, respectively (Fig 7B).

A

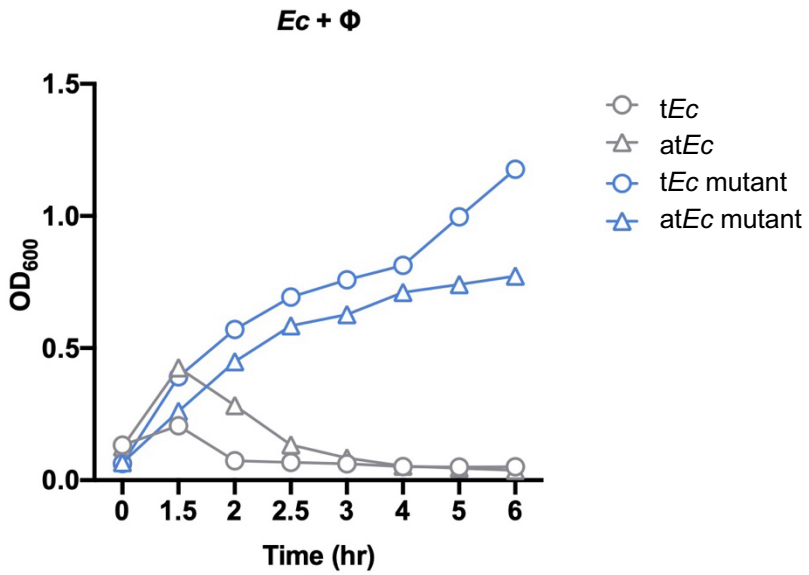

B

E. coli strain	Candidate receptor
t*Ec*	TonB-dependent vitamin B12 receptor BtuB
at*Ec*	Outer membrane protein C

Figure 7 Random Tn insertion mutants reveal candidate receptors. (A) Mutants selected from random transposon mutagenesis exhibited complete resistance to corresponding phages. (B) Putative host receptors used by each ϕt*Ec* and ϕat*Ec* were identified by sequencing the junction of the transposon insertion.

3. Escherichia coli strains exhibit tolerance to phages under reactive oxygen stress

High levels of ROS is one of the key characteristics of IBD gut environment[35, 40]. Using our model system of bacteriophage and gut commensal *E. coli* strains, we performed an infection experiment at various H_2O_2 concentrations and counted the number of viable cells at 3 h post infection. Increasing concentrations of H_2O_2 lowered the number of viable cells, with 2 mM H_2O_2 decreasing cell counts by ~2 log fold in both t*Ec* and at*Ec*, while 4 mM H_2O_2 killed all t*Ec* cells and decreased at*Ec* cell counts by ~4 log fold (Fig 8A). at*Ec* possesses one additional catalase, *eKatE*, which makes the strain more resistant to H_2O_2 than t*Ec*[39]. Phage-only treatment of the two strains resulted in ~5.5 log fold decrease of cell counts and complete killing of t*Ec* and at*Ec*, respectively (Fig 8A-B). Interestingly, however, when phage infection was initiated in the presence of 2 mM H_2O_2, and 2 mM and 4 mM H_2O_2 for t*Ec* and at*Ec*, respectively, the numbers of cells were comparable to that of H_2O_2-only treated bacteria. Presence of sufficiently high concentrations of H_2O_2 seemed to reduce the degree to which phages were able to lyse the host cells. Therefore, we suspected that ROS may be inducing phage-tolerant phenotype in the two *E. coli* strains.

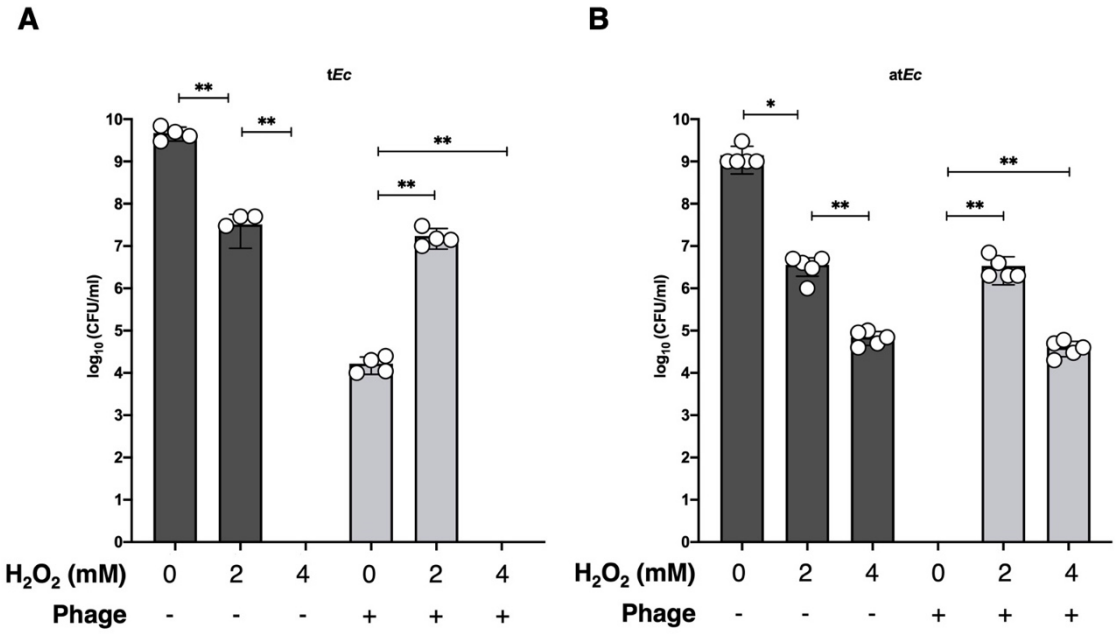

Figure 8 ROS-induced phage tolerance in *E. coli* . Phage infection assays of t*Ec* and at*Ec* under various H_2O_2 concentrations. Phage infection under H_2O_2 presence. ROS induced phage tolerance in (A) t*Ec* and (B) at*Ec*, $*P < 0.05$, $**P < 0.01$.

However, we wondered if the reduced lytic effect of the phage may be due to H_2O_2 inactivating the phages directly. We tested this possibility by first pre-treating the phages with H_2O_2 for 1 h, and subsequently adding catalase to the mixture to remove any remaining H_2O_2. These H_2O_2-pre-treated phages were then used to infect their respective *E. coli* hosts as in previous infection experiments, and again the number of viable cells were counted by plating. Interestingly, when phages were first treated with H_2O_2 and also catalase, phages exhibited no difference in their lytic activity, decreasing the cell numbers by ~6 log fold in both t*Ec* and at*Ec*, irrespective of the H_2O_2 concentration used (Fig 9A). However, when phages were only pre-treated with H_2O_2 and not catalase, such that host bacteria eventually became exposed to H_2O_2, phages were again only limitedly effective at host lysis. While phages not pre-treated with H_2O_2 significantly decreased the cell numbers by ~5 log fold and ~6.5 log fold in t*Ec* and at*Ec*, respectively, phages pre-treated with H_2O_2 were only able to decrease the cell numbers by ~2 log fold at 2 mM H_2O_2 and 4 mM H_2O_2 in t*Ec* and at*Ec*, respectively (Fig 9B). Based on these findings, we ruled out the possibility that H_2O_2 directly influences the phages' lytic activity.

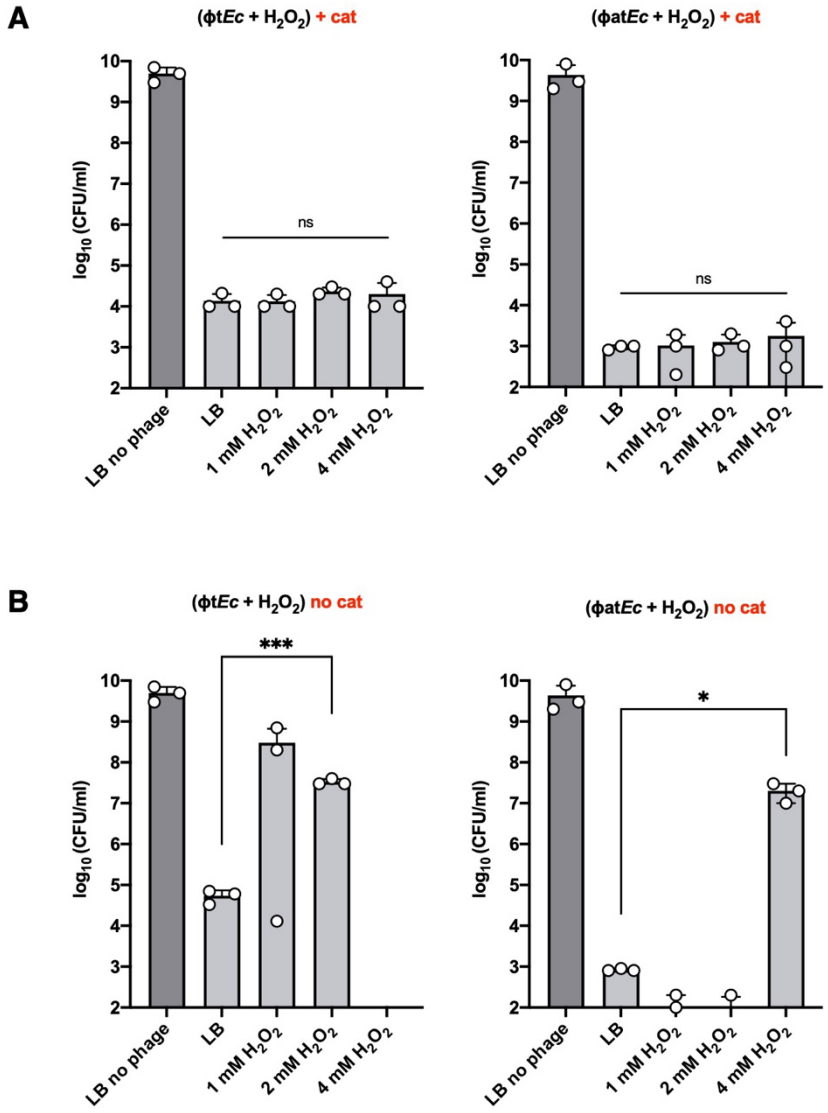

Figure 9 Phage pre-treatment with H_2O_2. (A) Viable cell counts after infection with phages pre-treated with varying concentrations of H_2O_2 and subsequent catalase to prevent *E. coli* from exposure to ROS show no reduced lytic activity. (B) Viable cell counts after infection with phages pre-treated with H_2O_2 but not catalase show reduced lytic activity. * $P < 0.05$, *** $P < 0.001$.

In contrast, the host *E. coli* strains seemed to be directly influenced by H_2O_2 treatment. When the two strains were treated with 1 mM and 2 mM H_2O_2, each strain showed a significant morphology change (Fig 10). At intermediate concentrations of H_2O_2, 1 mM for t*Ec* (Fig 10A) and 1 mM and 2 mM for at*Ec* (Fig 10B), both strains exhibited a slightly elongated cell shape. However, t*Ec* treated with 2 mM H_2O_2, which is the concentration that induced the phage-tolerant phenotype (Fig 8), cells exhibited a distinct wrinkled cell surface. While at*Ec* did not show this ruffled morphology at 2 mM, possibly due to its greater resistibility to ROS, we speculate that at a higher concentration such as 4 mM, a similar cell morphology to t*Ec* will be observed. Thus, we concluded that the ROS-induced phage-tolerance is due to a physiological change of the host bacteria, and not that of the phage.

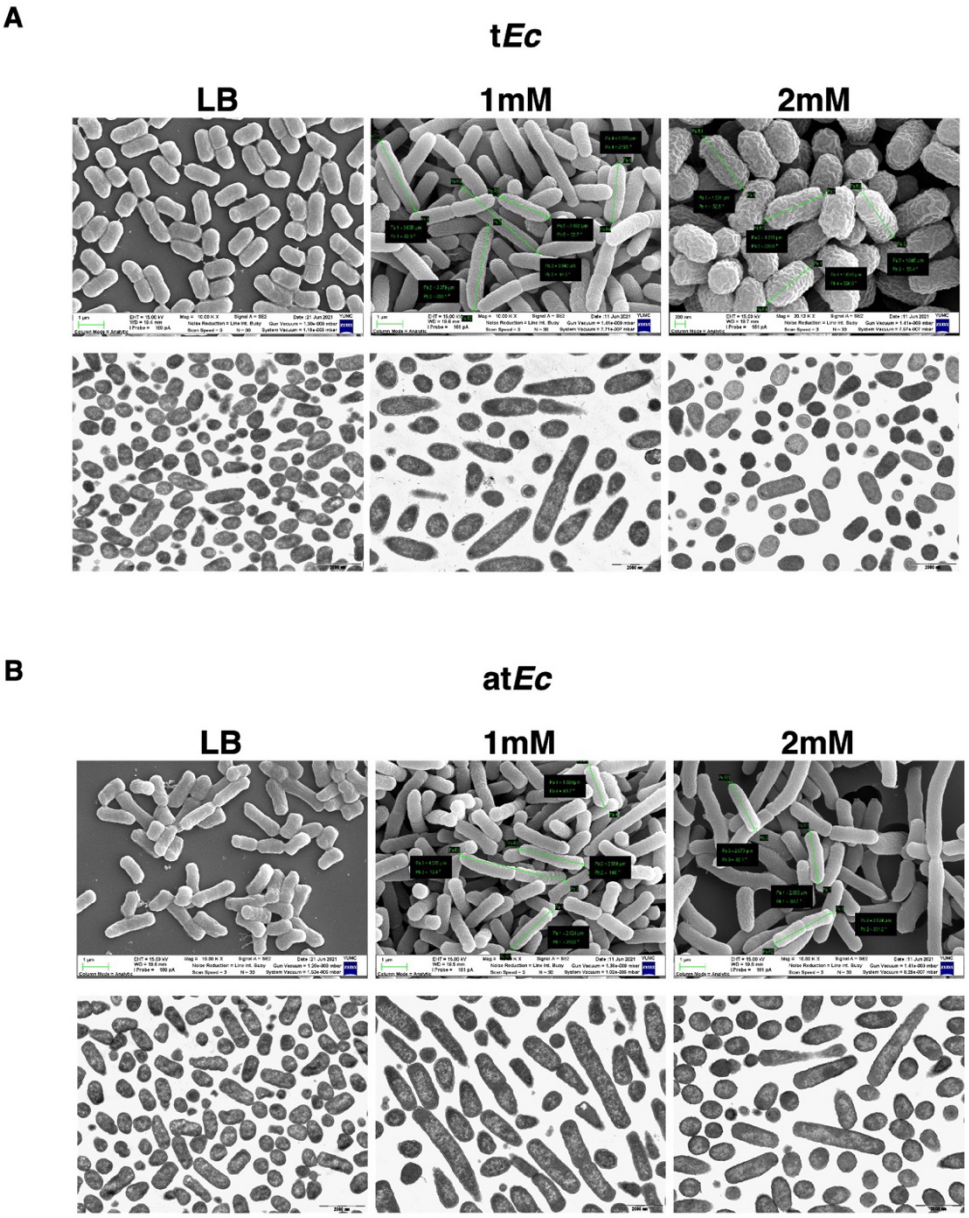

Figure 10 Electron micrographs of *E. coli* treated with H_2O_2. Electromicroscopy images of *E. coli* cells after H_2O_2 treatment (A) t*Ec* (B) at*Ec* reveal their cell morphologies are affected by ROS stress.

4. Concurrent reactive oxygen stress is necessary for phage tolerant phenotype

Next, we wondered whether concurrent ROS was required for phage tolerance or if pre-treatment with H_2O_2 prior to phage infection was sufficient for phage tolerance. *E. coli* were cultured in LB media supplemented with different concentrations of H_2O_2, for 1.5 h. Subsequently, cells were collected and resuspended in fresh LB media that contained phage only. While pre-treatment with increasing concentrations of H_2O_2 suppressed bacterial growth in the subsequent culture that excluded H_2O_2, phage-tolerant phenotype was not observed in groups that were infected with phage (Fig 11). Based on this finding, we concluded that simultaneous ROS presence is required for the bacteria to exhibit phage tolerance.

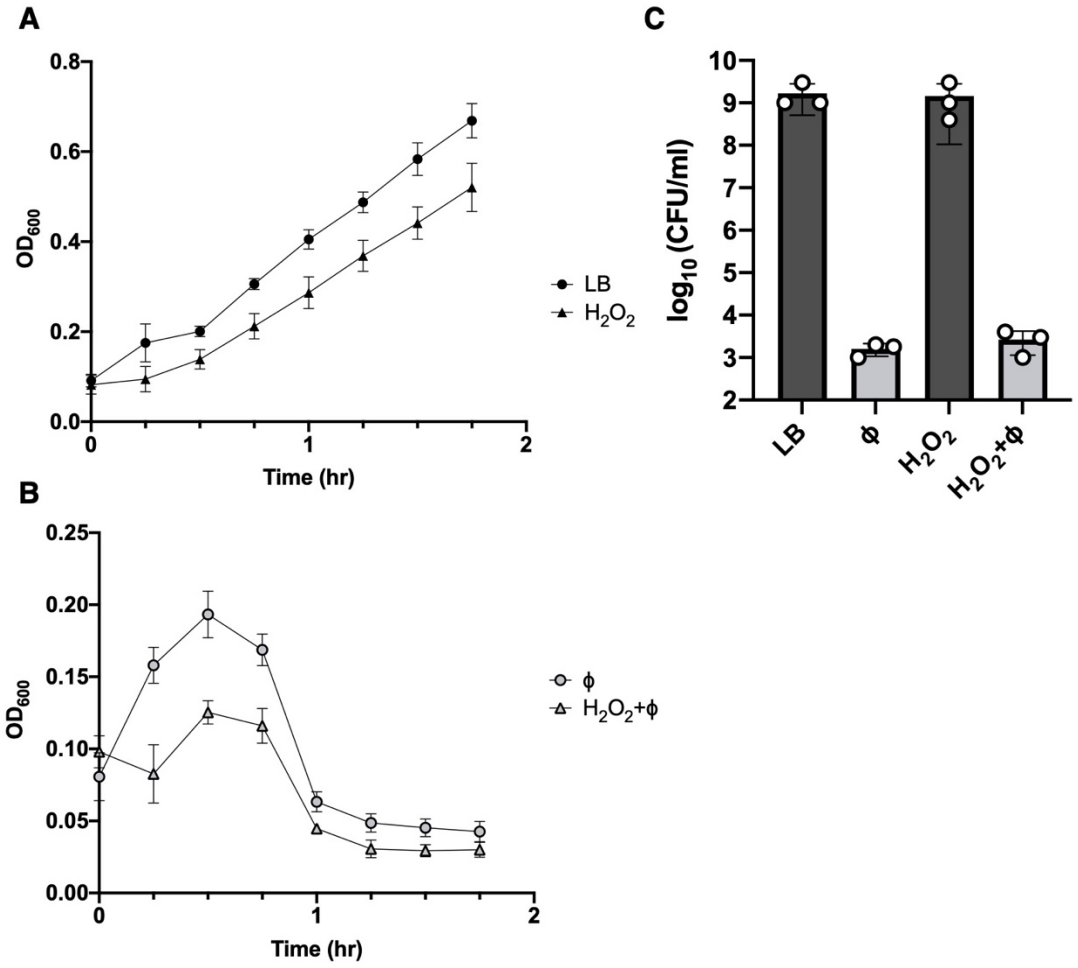

Figure 11 Simultaneous ROS stress is necessary for phage tolerance. Sequential addition of H_2O_2 and phages (A) Growth of H_2O_2-pre-treated t*Ec* cells grown subsequently in fresh LB media. (B) Lytic curves of H_2O_2-pre-treated t*Ec* cells (MOI=0.1) (C) Viable cell counts of H_2O_2-pre-treated t*Ec* cells infected with phage.

5. Tn-seq identifies susceptibility and resistance genes in phage killing

In order to identify the gene(s) responsible for ROS-induced phage tolerance, we performed transposon sequencing (Tn-seq) in t*Ec*. Using the mini Tn10 system, we created a high complexity Tn mutant library in t*Ec*. This library was cultured under 4 different conditions; LB (control), 8 mM H_2O_2 (ROS only), phage only, 8 mM H_2O_2 + phage (double stress). Similar to our previous infection experiments, surviving cells were collected and counted at 3 h post infection. Again, we observed phage tolerance in cells that were mixed with phage under the presence of H_2O_2 (Fig 12).

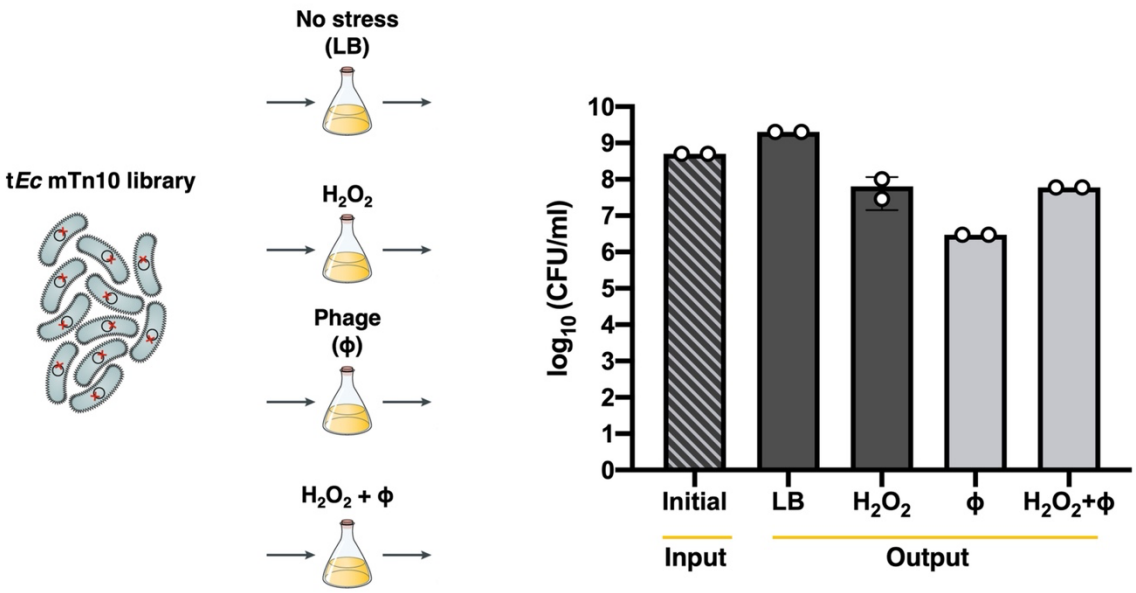

Figure 12 Schematic representation of Tn-seq design and viable cell counts of input and output. Highly complex t*Ec* mini Tn10 insertion mutant library was put through 4 different culture conditions to identify genes that are important for the ROS-induced phage tolerant phenotype. Viable cell counts verified that the libraries exhibited increased tolerance to phage when grown in the presence of ROS stress.

From these surviving cells, genomic DNA was extracted and subsequently prepared for sequencing of the transposon insertion junction. Analysis of the sequencing data revealed the lists of genes that confer either sensitivity or resistance under each stress conditions. In the phage only group, insertion mutants of *btuB* and *sdaC* exhibited significantly increased fitness under phage stress (Fig 13). These were predicted to be genes that encode the receptors that ϕt*Ec* uses to establish infection and reflects the finding from our random mutagenesis experiment (Fig 7). Indeed, when *btuB* was deleted, t*Ec* exhibited complete resistance to the phage (Fig 14A), and phage adsorption was completely blocked by *btuB* deletion (Fig 14B) indicating that BtuB is indeed a bona fide outer membrane receptor used by the phage. In the double stress group, 6 genes were predicted to confer tolerance to phage under presence of H_2O_2 (Fig 15). Thus, these genes most likely mediate the ROS-induced phage tolerance in t*Ec*.

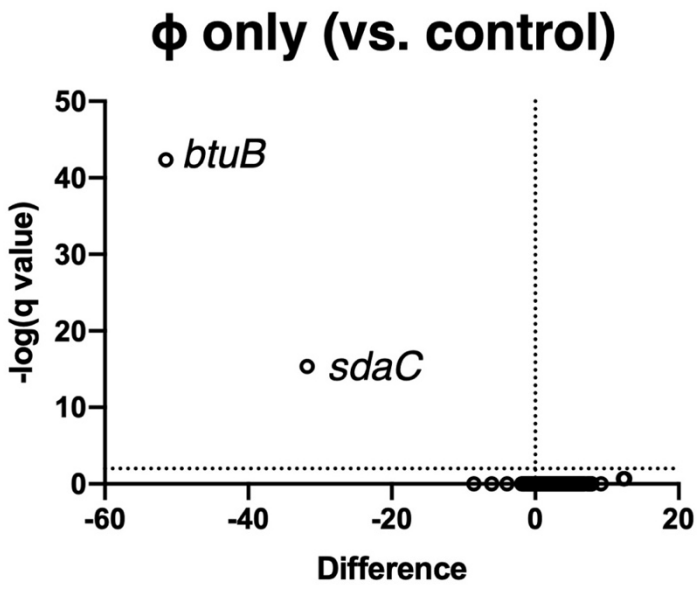

Gene	Annotation
btuB	Vitamin B12 receptor BtuB
sdaC	Serine transporter SdaC

Figure 13 Volcano plot of phage only treatment group. Phage only treatment group data exhibit two candidate genes that confer sensitivity to phage.

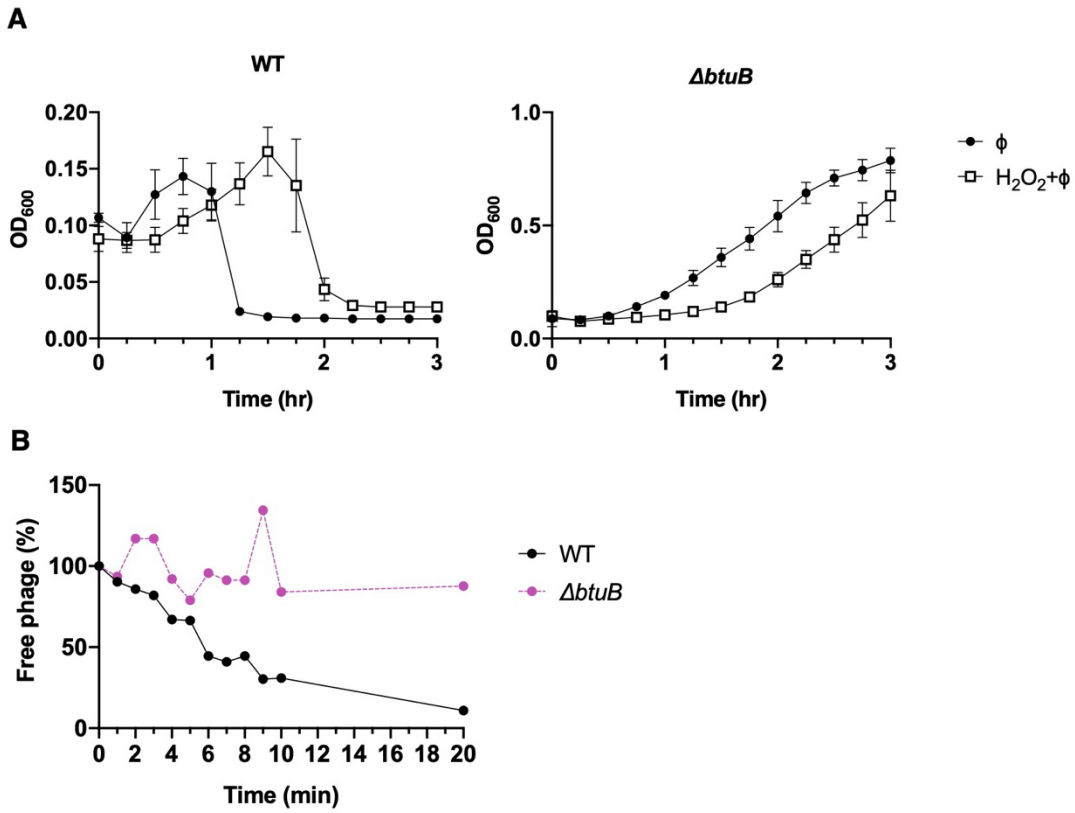

Figure 14 *btuB* deletion mutant exhibits complete inhibition of phage infection. (A) In-frame deletion mutant, *ΔbtuB*, exhibits complete resistance to ϕt*Ec*, regardless of H_2O_2 treatment. (B) Phage adsorption assay revealed that BtuB is indeed a host receptor molecule that enables phage adsorption, as *ΔbtuB* shows no adsorption over time.

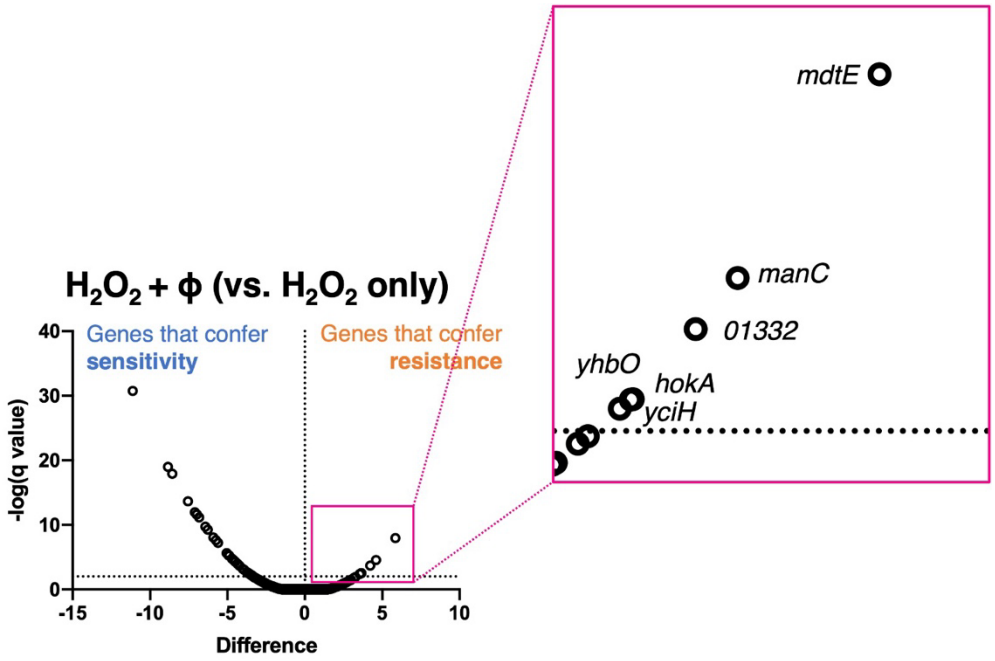

Gene	Annotation
mdtE	Multidrug resistance protein MdtE
manC	Mannose-1-phosphate guanylyltransferase
xisR	Prophage Rac excisionase
hokA	Small toxic peptide
yhbO	Protein/nucleic acid deglycase 2
yciH	putative protein YciH

Figure 15 Volcano plot of H_2O_2+phage treatment group. H_2O_2+phage treatment group data revealed 6 candidate genes that confer resistance to phage.

6. Deletion mutants exhibit decreased phage tolerance compared to wild type under ROS stress

In order to experimentally validate that the candidate genes predicted to confer phage tolerance under ROS stress do indeed confer protection, we performed a competition assay. First, we generated in-frame deletion mutants of 4 candidate genes as well as a *lacZ* deletion mutant to perform blue-white colony screening. Next, we co-cultured the strains with wild type cells under the same condition as Tn-seq, with or without the presence of ROS stress and/or phage. When we counted the number of surviving cells, we noticed that the deletion mutants exhibited decreased fitness (Fig 16), as evidenced by their competitive indices (indices smaller than 1 signal reduced fitness compared to wild type). Thus, this data supports that the deletion of these genes leads to fitness defect of the cells when subjected to phage attack and concurrent ROS stress.

In order to examine the transcription levels of these tolerance genes under oxidative stress, t*Ec* cells were treated with H_2O_2 and RNA was extracted from these cells. RT-qPCR data revealed that transcription level of all of the 6 target genes except for *yhbO* were either maintained at the same level or slightly upregulated upon H_2O_2 treatment compared to control (Fig 16B). Especially, *manC* gene involved in colanic acid capsule biosynthesis and *yciH* encoding a putative protein were shown to be significantly upregulated. This data corroborates RNA sequencing data, as most of the tolerance genes were shown to be transcriptionally upregulated (Fig 16A), while *yciH* was most robustly

upregulated. Hence, this indicates that the tolerance genes are most likely to be transcriptionally active during oxidative stress condition induced by H_2O_2, and that their active transcriptional status enables the gene products in facilitating phage tolerance under ROS condition.

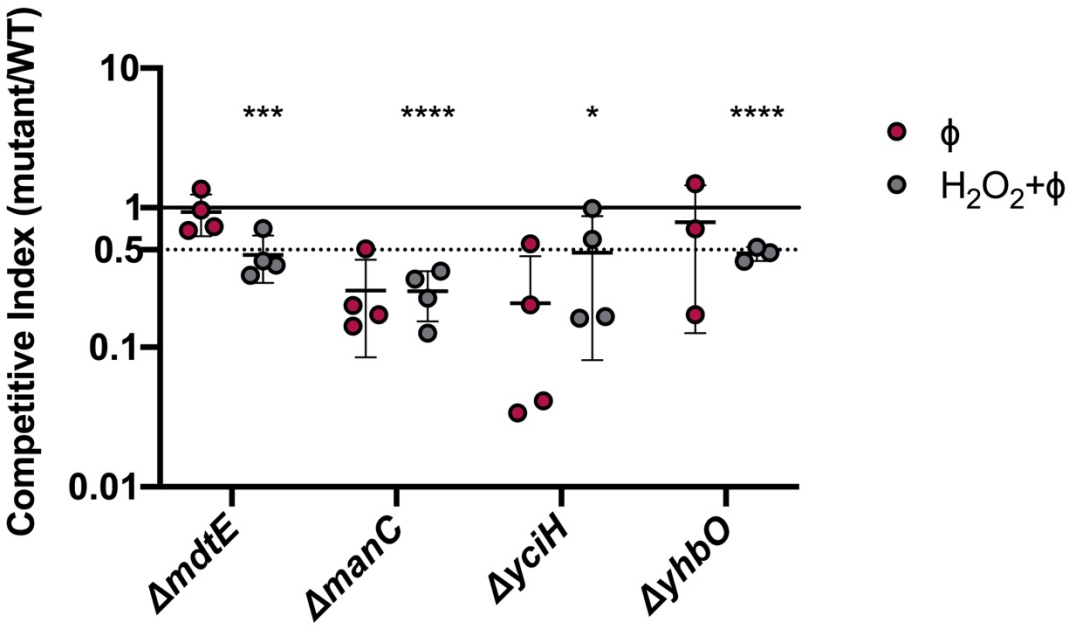

Figure 16 Experimental validation of deletion mutants via competition assay. Competitive indices indicate the fitness of each strain relative to the wild type t*Ec*. Deletion mutants exhibited loss of ROS-induced phage tolerance.

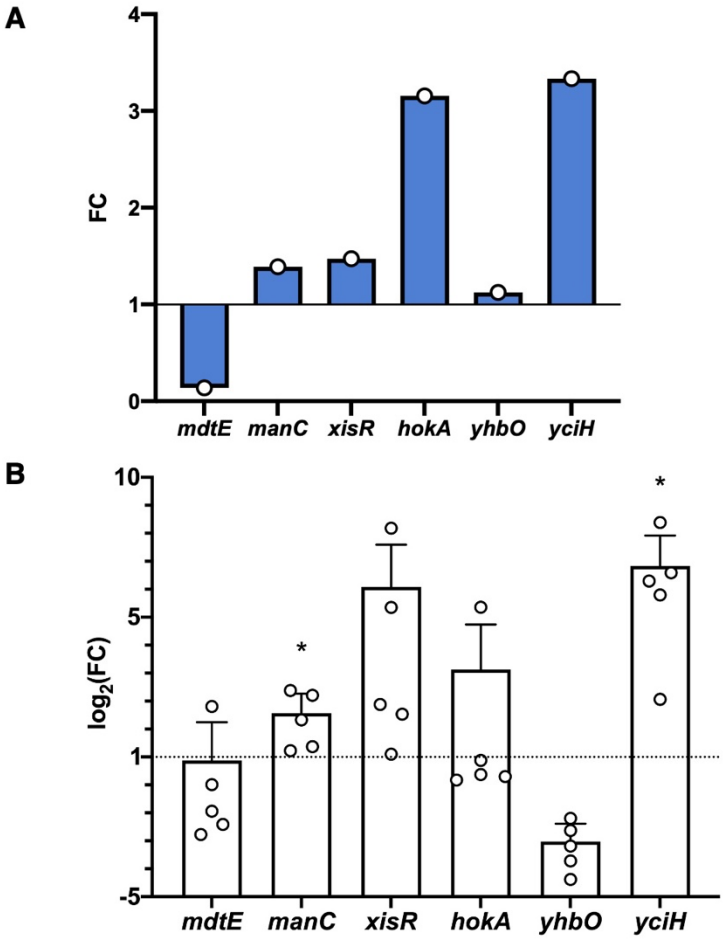

Figure 17 Transcription levels of candidate phage resistance genes in H_2O_2-treated t*Ec* cells. (A) RNA sequencing revealed that transcriptions of most target genes, except for *mdtE*, are slightly upregulated, especially for *hokA* and *yciH* with greater than 2-fold increases. (B) Real-time quantitative PCR similarly showed that gene expression is upregulated for most genes when cells were subjected to oxidative stress by H_2O_2 and especially significantly for *manC* and *yciH*. Data points were collected from 5 biological replicates. *$P < 0.05$.

IV. DISCUSSION

In our model system of gut commensal *E. coli* isolates and their bacteriophages under the presence of ROS, phage-bacteria interactions were closely investigated. Most notably, the gut *E. coli* isolates exhibited increased tolerance to phage under ROS (Fig 8), while ROS in and of itself did not seem to influence the phages' ability to complete lysis (Fig 9). Moreover, phage tolerant phenotype was observed only when the bacterial cells were exposed to a simultaneous and sufficiently high level of ROS (Fig 10). Based on these findings, we speculated that ROS induces a physiological change in the host bacteria, which confers increased tolerance to phage.

Transposon sequencing (Tn-seq) of the t*Ec* strain revealed potential genes that confer sensitivity or tolerance to phage. When the transposon mutant library was passaged in the presence of phage, with the two most relevant gene hits identified as *btuB* and *sdaC*, encoding vitamin B12 receptor BtuB and serine transporter SdaC, respectively (Fig 13). Detection of btuB mirrors the random transposon mutagenesis results, where insertion in the *btuB* gene was similarly found to confer resistance to phage infection (Fig 7). We suspect that BtuB is the outer membrane receptor that the phage uses, as multiple phages have been reported to use it to establish adsorption[49]. Additionally, Tn-seq uncovered SdaC, most likely the inner membrane receptor that the phage uses. SdaC have been reported to be

the secondary receptor that phages utilize in combination with the primary receptor BtuB, in order to inject their DNA into host cell[49]. Given our promising results in detecting what genes are relevant for t*Ec* under phage infection pressure, we investigated into which genes may be conferring the phage tolerance phenotype under ROS condition. For this, we compared the fitness of mutants between two conditions, ROS+ϕ (double stress) and ROS only. Using a stringent cutoff of q-value > 0.001 , our analysis revealed 6 candidate genes - *mdtE, manC, xisR, hokA, yhbO, yciH* - that seem to confer tolerance to phage in ROS culture condition (Fig 15). Based on our RT-qPCR data, manC and yciH were significantly upregulated, RNA sequencing results, all genes except for *mdtE* exhibited increased transcription levels in the double stress condition (Fig 17B). This highlights the likelihood of expression of these genes getting induced by H_2O_2 and thus facilitating ROS-induced phage tolerance.

Based on previous research, we speculate, as follows, how the identified candidate resistance genes might be conferring ROS-induced phage tolerance (Fig 18):

Firstly, *hokA* encodes the peptide toxin of a type I toxin-antitoxin system. One of the immune mechanisms that bacteria use against phage attack is abortive infection mediated through toxin-antitoxin systems[50]. Under normal conditions, *hokA* mRNA is bound by the corresponding *sok* antitoxin mRNA, such that *hokA* translation is suppressed. However, if *hokA* translation is somehow increased,

HokA toxins produced can result in programmed cell death[51]. In phage-infected bacterial cells, HokA activation results in “altruistic suicide” and its death effectively prevents production of more phage particles and saves the bacterial population.

Secondly, *xisR* encodes excisionase and is part of prophage Rac within the t*Ec* genome. XisR is required for the prophage’s excision from the host genome and entering the lytic replication cycle[52]. Prophages are known to mediate defense against phage infections through various mechanisms[53]. While the exact role of excisionase in conferring resistance to a lytic phage superinfection is unknown, we speculate that prophage induction during lytic phage infection can lead to loss of host cell viability and thus unsuccessful replication of the lytic phage.

Thirdly, *manC* encodes mannose-1-phosphate guanylyltrasnferase, which is involved in colanic acid biosynthesis and capsule formation. While there are some phages that recognize and specifically bind to the bacterial capsule for establishing adsorption, for other phages the capsule may function as a resistance mechanism[54-57]. In the latter case, the capsule is a protective layer against the bacteriophage, physically obstructing the phage from getting into proximity with the host and binding to its receptor[56]. Thus, since ϕt*Ec* uses the BtuB protein for receptor (Fig 7B), the capsule most likely confers resistance against the phage to t*Ec*.

Forthly, *mdtE* encodes a multidrug efflux pump protein belonging to the resistance nodulation division (RND) family. Multidrug efflux pump proteins

have been reported to be receptors recognized by phages and important for adsorption[58, 59] or known to confer antibiotic resistance to bacteria through efflux of the drugs[60-62]. However, multidrug efflux pumps can export a wide range of substrates, ranging from bacterial toxins[60, 63, 64] and chemicals[61] to host-derived substances such as bile salts and hormones[65]. Especially, bacterial toxins such as hemolysin and colicin are also exported into the extracellular space through multidrug efflux pumps[63, 64]. Presently, no research has yet reported MdtE or any other multidrug efflux pump's specificity for exporting phage-derived toxins. However, given the relatively small size of phage-derived toxins compared to bacterial toxins, it seems not all too impossible that there exists a multidrug efflux pump that exports phage-derived toxins such as endolysin and holin. While this speculation needs thorough validation, I speculate that MdtE may be a novel tolerance mechanism against phage under oxidative stress condition, by exporting phage-derived toxins, and thus inhibiting lysis of the host cell.

Fifthly, *yhbO* encodes a protein/nucleic acid deglycase, involved in repair of glycated protein and glycated nucleic acid. YhbO is a general stress protein that plays an important role in oxidative stress condition, as oxidative stress results in glycation damage and cellular dysfunction in consequence[66, 67]. No phage tolerance mechanism directly involving YhbO has been reported yet, while it is possible that inability to appropriately repair glycated proteins that themselves play a role in mediating phage tolerance would hinder the bacterial cell more susceptible to phage attack. Thus, YhbO may be functioning indirectly through

repair of agents that are involved in phage tolerance in oxidative stress.

Lastly, *yciH* encodes a putative stress response regulator. It has been reported that YciH regulates the expression of stress-related genes and significantly decreased the production of their gene products[68]. Again, similar to YhbO, as a general stress response protein, under oxidative stress condition, YciH may be modulating specific downstream activities that additionally confer phage tolerance.

While previously no specific association of *yciH* has been made with phage infection, it may be possible that YciH moderates change in the t*Ec* membrane that is associated with stress response, such that it is more resistant to phage lysis.

In response to H_2O_2, t*Ec* transcriptomic profile revealed increased transcription of *soxRS* but not *oxyR* genes (data not shown). Genes in the *soxRS* regulon, such as *sodA* encoding superoxide dismutase were upregulated. Notably, increased levels of transcription were observed for all candidate genes except for *mdtE*, in H_2O_2-treated t*Ec*. (Fig 17A). These results are in alignment with the quantitative PCR data, as most genes showed a trend of upregulated expression, with *manC* and *yciH* being significantly upregulated (Fig 17B). These data collectively support the likelihood these genes' importance in effecting the *E. coli*'s physiological changes in response to ROS, and thereby conferring ROS-induced phage tolerance.

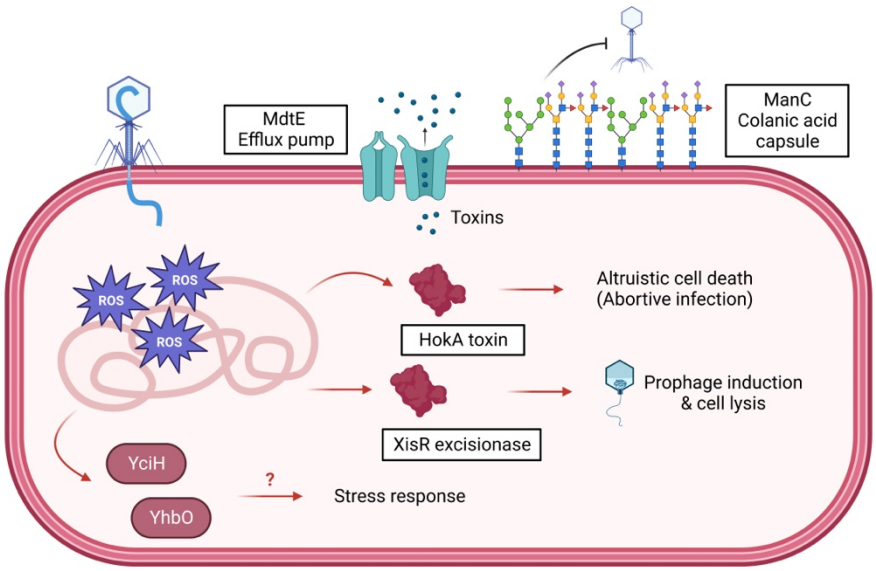

Figure 18 Proposed mechanism of tolerance. Diagram summarizes how each gene product may confer tolerance to lysis by phage.

While expansion of the *E. coli* population in inflammatory bowel disease (IBD) gut environment is a widely acknowledged fact [28-30], it remains unclear how the bacterial population interacts with their counterpart bacteriophage population. It is also yet unclear how such interactions shape the progression of the disease. This study aimed to investigate how gut commensal *E. coli* isolates interact with their bacteriophages, in a condition that mimics inflammatory bowel disease (IBD) gut environment. Our findings that *E. coli* react to ROS in such ways that they become more phage-tolerant add new knowledge to what we know about *E. coli*-phage interactions. We hypothesize that this ROS-induced phage tolerance is what enables the uncontrolled propagation of *E. coli* in the IBD gut environment (Fig 19). Furthermore, since aborted phage infections that do not result in phage replication leads to loss of infective phage material and therefore may result in a decreased collective infective capacity of phages, this phenotype also may cause a decline in the number of *E. coli*-targeting phages in the gut. This reduced phage population can thereby feed into the cycle and exacerbate the *Enterobacteriaceae* bloom in the gut and inflammation.

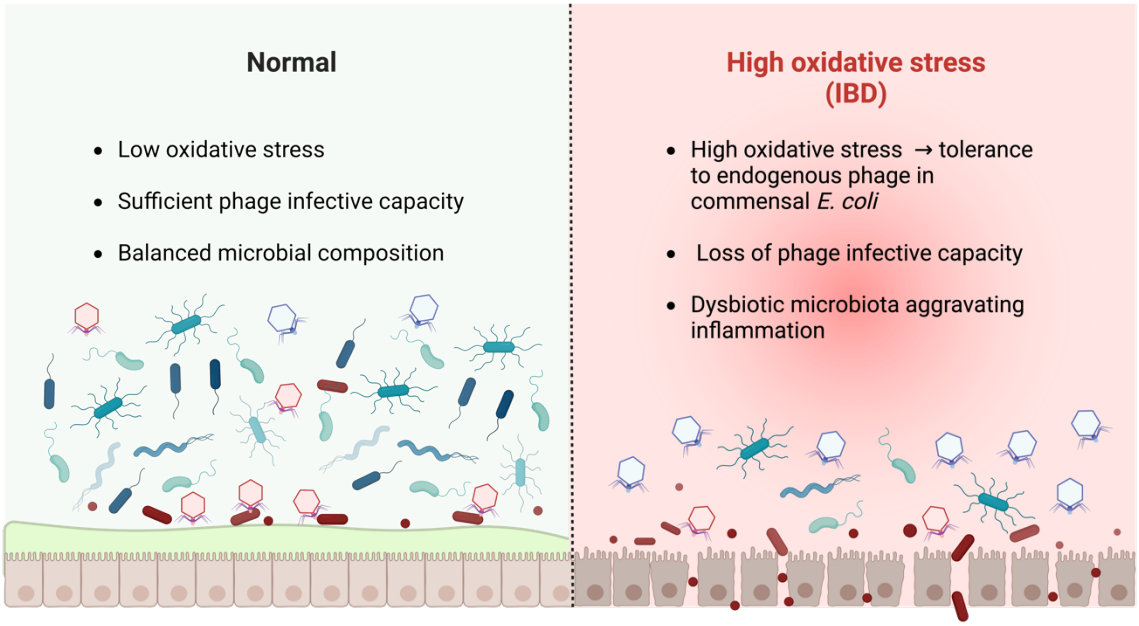

Figure 19 Proposed *E. coli* – bacteriophage interactions underlying IBD. Under normal condition, low oxygen potential in the gut allows maintenance of sufficient phage infective capacity and eubiosis. Under high oxidative stress condition as in IBD, *E. coli* may become tolerant to the endogenous gut phages, and hence result in loss of phage infective capacity, which in turn aggravates the dysbiotic proliferation of E. coli and inflammation in consequence.

Finally, phages are potentially very important therapeutic tools in treatment of microbiome-associated diseases, including IBD. However, with the ROS-induced phage tolerant phenotype of *E. coli* that we observed in this study in mind, future research may investigate if administration of drugs such as anti-inflammatory drugs for lowering the level of ROS or molecules that can revert or impede the ROS-induced changes of *E. coli* such that they are more phage susceptible, in combination with phage therapy results in greater therapeutic efficacy.

V. CONCLUSION

In this study, we hypothesized that interactions between gut commensal *E. coli* and bacteriophage might be a contributing factor to the dysbiotic expansion of the *E. coli* population in inflammatory environment such as the IBD gut. For this, we established a model system of two gut commensal *E. coli* isolate strains, previously shown to be well-adapted to surviving in the high ROS environment, and lytic phages that can target these two strains. Interestingly, we observed that ROS induced a phage tolerant phenotype in the two gut commensal *E. coli* strains, through H_2O_2-mediated physiological changes of the bacteria, and not due to changes of phages. Transposon sequencing successfully identified genes that confer sensitivity to phage, as well as ROS-mediated phage tolerance. Further experimental validation of deletion mutant phenotype is required to verify the involvement of the identified genes in facilitating phage tolerance.

REFERENCES

1. Lopez-Garcia P, Gutierrez-Preciado A, Krupovic M, et al. Metagenome-derived virus-microbe ratios across ecosystems. ISME J. May 11 2023;doi:10.1038/s41396-023-01431-y
2. Malki K, Rosario K, Sawaya NA, Szekely AJ, Tisza MJ, Breitbart M. Prokaryotic and Viral Community Composition of Freshwater Springs in Florida, USA. mBio. Apr 7 2020;11(2)doi:10.1128/mBio.00436-20
3. Srinivasiah S, Bhavsar J, Thapar K, Liles M, Schoenfeld T, Wommack KE. Phages across the biosphere: contrasts of viruses in soil and aquatic environments. Res Microbiol. Jun 2008;159(5):349-57. doi:10.1016/j.resmic.2008.04.010
4. Suttle CA. Viruses in the sea. Nature. Sep 15 2005;437(7057):356-61. doi:10.1038/nature04160
5. Zuppi M, Hendrickson HL, O'Sullivan JM, Vatanen T. Phages in the Gut Ecosystem. Front Cell Infect Microbiol. 2021;11:822562. doi:10.3389/fcimb.2021.822562
6. Al-Shayeb B, Sachdeva R, Chen LX, et al. Clades of huge phages from across Earth's ecosystems. Nature. Feb 2020;578(7795):425-431. doi:10.1038/s41586-020-2007-4
7. Gonzalez B, Monroe L, Li K, et al. Phage G Structure at 6.1 A

Resolution, Condensed DNA, and Host Identity Revision to a Lysinibacillus. J Mol Biol. Jun 26 2020;432(14):4139-4153. doi:10.1016/j.jmb.2020.05.016

8. Suhanovsky MM, Teschke CM. Nature's favorite building block: Deciphering folding and capsid assembly of proteins with the HK97-fold. Virology. May 2015;479-480:487-97. doi:10.1016/j.virol.2015.02.055

9. Daugelavicius R, Cvirkaite V, Gaidelyte A, Bakiene E, Gabrenaite-Verkhovskaya R, Bamford DH. Penetration of enveloped double-stranded RNA bacteriophages phi13 and phi6 into Pseudomonas syringae cells. J Virol. Apr 2005;79(8):5017-26. doi:10.1128/JVI.79.8.5017-5026.2005

10. Wei H, Cheng RH, Berriman J, et al. Three-dimensional structure of the enveloped bacteriophage phi12: an incomplete T = 13 lattice is superposed on an enclosed T = 1 shell. PLoS One. Sep 3 2009;4(9):e6850. doi:10.1371/journal.pone.0006850

11. Young R. Phage lysis: three steps, three choices, one outcome. J Microbiol. Mar 2014;52(3):243-58. doi:10.1007/s12275-014-4087-z

12. Nanda AM, Thormann K, Frunzke J. Impact of spontaneous prophage induction on the fitness of bacterial populations and

host-microbe interactions. J Bacteriol. Feb 2015;197(3):410-9. doi:10.1128/JB.02230-14

13. Feiner R, Argov T, Rabinovich L, Sigal N, Borovok I, Herskovits AA. A new perspective on lysogeny: prophages as active regulatory switches of bacteria. Nat Rev Microbiol. Oct 2015;13(10):641-50. doi:10.1038/nrmicro3527

14. Hartley MA, Ronet C, Fasel N. Backseat drivers: the hidden influence of microbial viruses on disease. Curr Opin Microbiol. Aug 2012;15(4):538-45. doi:10.1016/j.mib.2012.05.011

15. Hobbs Z, Abedon ST. Diversity of phage infection types and associated terminology: the problem with 'Lytic or lysogenic'. FEMS Microbiol Lett. Apr 2016;363(7)doi:10.1093/femsle/fnw047

16. Principi N, Silvestri E, Esposito S. Advantages and Limitations of Bacteriophages for the Treatment of Bacterial Infections. Front Pharmacol. 2019;10:513. doi:10.3389/fphar.2019.00513

17. Royer S, Morais AP, da Fonseca Batistao DW. Phage therapy as strategy to face post-antibiotic era: a guide to beginners and experts. Arch Microbiol. May 2021;203(4):1271-1279. doi:10.1007/s00203-020-02167-5

18. Gu Liu C, Green SI, Min L, et al. Phage-Antibiotic Synergy Is Driven by a Unique Combination of Antibacterial Mechanism of

Action and Stoichiometry. mBio. Aug 4 2020;11(4)doi:10.1128/mBio.01462-20

19. Racenis K, Lacis J, Rezevska D, et al. Successful Bacteriophage-Antibiotic Combination Therapy against Multidrug-Resistant Pseudomonas aeruginosa Left Ventricular Assist Device Driveline Infection. Viruses. May 20 2023;15(5)doi:10.3390/v15051210

20. Machiels K, Joossens M, Sabino J, et al. A decrease of the butyrate-producing species Roseburia hominis and Faecalibacterium prausnitzii defines dysbiosis in patients with ulcerative colitis. Gut. Aug 2014;63(8):1275-83. doi:10.1136/gutjnl-2013-304833

21. Paik D, Yao L, Zhang Y, et al. Human gut bacteria produce Tau(Eta)17-modulating bile acid metabolites. Nature. Mar 2022;603(7903):907-912. doi:10.1038/s41586-022-04480-z

22. Benler S, Yutin N, Antipov D, et al. Thousands of previously unknown phages discovered in whole-community human gut metagenomes. Microbiome. Mar 29 2021;9(1):78. doi:10.1186/s40168-021-01017-w

23. Camarillo-Guerrero LF, Almeida A, Rangel-Pineros G, Finn RD, Lawley TD. Massive expansion of human gut bacteriophage diversity. Cell. Feb 18 2021;184(4):1098-1109 e9.

doi:10.1016/j.cell.2021.01.029

24. Moreno-Gallego JL, Chou SP, Di Rienzi SC, et al. Virome Diversity Correlates with Intestinal Microbiome Diversity in Adult Monozygotic Twins. Cell Host Microbe. Feb 13 2019;25(2):261-272 e5. doi:10.1016/j.chom.2019.01.019

25. Hsu BB, Gibson TE, Yeliseyev V, et al. Dynamic Modulation of the Gut Microbiota and Metabolome by Bacteriophages in a Mouse Model. Cell Host Microbe. Jun 12 2019;25(6):803-814 e5. doi:10.1016/j.chom.2019.05.001

26. Gogokhia L, Buhrke K, Bell R, et al. Expansion of Bacteriophages Is Linked to Aggravated Intestinal Inflammation and Colitis. Cell Host Microbe. Feb 13 2019;25(2):285-299 e8. doi:10.1016/j.chom.2019.01.008

27. Norman JM, Handley SA, Baldridge MT, et al. Disease-specific alterations in the enteric virome in inflammatory bowel disease. Cell. Jan 29 2015;160(3):447-60. doi:10.1016/j.cell.2015.01.002

28. Baldelli V, Scaldaferri F, Putignani L, Del Chierico F. The Role of Enterobacteriaceae in Gut Microbiota Dysbiosis in Inflammatory Bowel Diseases. Microorganisms. Mar 27 2021;9(4)doi:10.3390/microorganisms9040697

29. Garrett WS, Gallini CA, Yatsunenko T, et al. Enterobacteriaceae

act in concert with the gut microbiota to induce spontaneous and maternally transmitted colitis. Cell Host Microbe. Sep 16 2010;8(3):292-300. doi:10.1016/j.chom.2010.08.004

30. Lloyd-Price J, Arze C, Ananthakrishnan AN, et al. Multi-omics of the gut microbial ecosystem in inflammatory bowel diseases. Nature. May 2019;569(7758):655-662. doi:10.1038/s41586-019-1237-9

31. De Sordi L, Lourenco M, Debarbieux L. The Battle Within: Interactions of Bacteriophages and Bacteria in the Gastrointestinal Tract. Cell Host Microbe. Feb 13 2019;25(2):210-218. doi:10.1016/j.chom.2019.01.018

32. Shkoporov AN, Turkington CJ, Hill C. Mutualistic interplay between bacteriophages and bacteria in the human gut. Nat Rev Microbiol. Dec 2022;20(12):737-749. doi:10.1038/s41579-022-00755-4

33. Johnson LA, Hug LA. Distribution of reactive oxygen species defense mechanisms across domain bacteria. Free Radic Biol Med. Aug 20 2019;140:93-102. doi:10.1016/j.freeradbiomed.2019.03.032

34. Bourgonje AR, von Martels JZH, Bulthuis MLC, et al. Crohn's Disease in Clinical Remission Is Marked by Systemic Oxidative

Stress. Front Physiol. 2019;10:499. doi:10.3389/fphys.2019.00499

35. Bourgonje AR, Feelisch M, Faber KN, Pasch A, Dijkstra G, van Goor H. Oxidative Stress and Redox-Modulating Therapeutics in Inflammatory Bowel Disease. Trends Mol Med. Nov 2020;26(11):1034-1046. doi:10.1016/j.molmed.2020.06.006

36. Chanin RB, Winter MG, Spiga L, et al. Epithelial-Derived Reactive Oxygen Species Enable AppBCX-Mediated Aerobic Respiration of Escherichia coli during Intestinal Inflammation. Cell Host Microbe. Dec 9 2020;28(6):780-788 e5. doi:10.1016/j.chom.2020.09.005

37. Albenberg L, Esipova TV, Judge CP, et al. Correlation between intraluminal oxygen gradient and radial partitioning of intestinal microbiota. Gastroenterology. Nov 2014;147(5):1055-63 e8. doi:10.1053/j.gastro.2014.07.020

38. Litvak Y, Byndloss MX, Tsolis RM, Baumler AJ. Dysbiotic Proteobacteria expansion: a microbial signature of epithelial dysfunction. Curr Opin Microbiol. Oct 2017;39:1-6. doi:10.1016/j.mib.2017.07.003

39. Yoon MY, Min KB, Lee KM, et al. A single gene of a commensal microbe affects host susceptibility to enteric infection. Nat Commun. May 13 2016;7:11606. doi:10.1038/ncomms11606

40. Tian T, Wang Z, Zhang J. Pathomechanisms of Oxidative Stress in Inflammatory Bowel Disease and Potential Antioxidant Therapies. Oxid Med Cell Longev. 2017;2017:4535194. doi:10.1155/2017/4535194

41. Martin M. Cutadapt Removes Adapter Sequences From High-Throughput Sequencing Reads. EMBnetjournal. 2011;17(1):10-12. doi:10.14806/ej.17.1.200

42. Bankevich A, Nurk S, Antipov D, et al. SPAdes: a new genome assembly algorithm and its applications to single-cell sequencing. J Comput Biol. May 2012;19(5):455-77. doi:10.1089/cmb.2012.0021

43. Seemann T. Prokka: rapid prokaryotic genome annotation. Bioinformatics. Jul 15 2014;30(14):2068-9. doi:10.1093/bioinformatics/btu153

44. Arndt D, Grant JR, Marcu A, et al. PHASTER: a better, faster version of the PHAST phage search tool. Nucleic Acids Res. Jul 8 2016;44(W1):W16-21. doi:10.1093/nar/gkw387

45. Grant JR, Enns E, Marinier E, et al. Proksee: in-depth characterization and visualization of bacterial genomes. Nucleic Acids Res. May 4 2023;doi:10.1093/nar/gkad326

46. Lazinski DW, Camilli A. Homopolymer tail-mediated ligation PCR:

a streamlined and highly efficient method for DNA cloning and library construction. Biotechniques. Jan 2013;54(1):25-34. doi:10.2144/000113981

47. McDonough E, Lazinski DW, Camilli A. Identification of in vivo regulators of the Vibrio cholerae xds gene using a high-throughput genetic selection. Mol Microbiol. Apr 2014;92(2):302-15. doi:10.1111/mmi.12557

48. Shull LM, Camilli A. Transposon Sequencing of Vibrio cholerae in the Infant Rabbit Model of Cholera. Methods Mol Biol. 2018;1839:103-116. doi:10.1007/978-1-4939-8685-9_10

49. Valery V. Samsonov VVS, Sergey P. Sineoky. DcrA and dcrB Escherichia coli genes can control DNA injection
by phages specific for BtuB and FhuA receptors. Research in Microbiology. 2002;153 639-646.

50. Song S, Wood TK. A Primary Physiological Role of Toxin/Antitoxin Systems Is Phage Inhibition. Front Microbiol. 2020;11:1895. doi:10.3389/fmicb.2020.01895

51. Pedersen K, Gerdes K. Multiple hok genes on the chromosome of Escherichia coli. Mol Microbiol. Jun 1999;32(5):1090-102. doi:10.1046/j.1365-2958.1999.01431.x

52. Liu X, Li Y, Guo Y, et al. Physiological Function of Rac Prophage

During Biofilm Formation and Regulation of Rac Excision in Escherichia coli K-12. Sci Rep. Nov 4 2015;5:16074. doi:10.1038/srep16074

53. Bondy-Denomy J, Qian J, Westra ER, et al. Prophages mediate defense against phage infection through diverse mechanisms. ISME J. Dec 2016;10(12):2854-2866. doi:10.1038/ismej.2016.79

54. Mangalea MR, Duerkop BA. Fitness Trade-Offs Resulting from Bacteriophage Resistance Potentiate Synergistic Antibacterial Strategies. Infect Immun. Jun 22 2020;88(7)doi:10.1128/IAI.00926-19

55. Fehmel FF, U.; Niemann, H.; Stirm, S. Escherichia coli Capsule Bacteriophages. Journal of Virology. September 1975 1975:591-601. doi:10.1128/JVI.16.3.591-601.1975

56. Soundararajan M, von Bunau R, Oelschlaeger TA. K5 Capsule and Lipopolysaccharide Are Important in Resistance to T4 Phage Attack in Probiotic E. coli Strain Nissle 1917. Front Microbiol. 2019;10:2783. doi:10.3389/fmicb.2019.02783

57. Wilkinson BJH, K. M. Staphylococcus aureus Cell Surface: Capsule as a Barrier to Bacteriophage Adsorption. Infection and Immunity. 1979;23(2):549-552. doi:10.1128/iai.23.2.549-552.1979

58. Esteves NCP, S.; McClelland, M.; Scharf, B. E. The Multidrug

Efflux System AcrABZ-TolC Is Essential for
Infection of Salmonella Typhimurium by the Flagellum-
Dependent Bacteriophage Chi. J virol. 2021;95:e00394-21. doi:10.1128/JVI.00394

59. Koderi Valappil S, Shetty P, Deim Z, et al. Survival Comes at a Cost: A Coevolution of Phage and Its Host Leads to Phage Resistance and Antibiotic Sensitivity of Pseudomonas aeruginosa Multidrug Resistant Strains. Front Microbiol. 2021;12:783722. doi:10.3389/fmicb.2021.783722

60. Huang L, Wu C, Gao H, et al. Bacterial Multidrug Efflux Pumps at the Frontline of Antimicrobial Resistance: An Overview. Antibiotics (Basel). Apr 13 2022;11(4)doi:10.3390/antibiotics11040520

61. Piddock L. Multidrug-resistance efflux pumps - not just for resistance. Nat Rev Microbiol. 2006;4:629-636. doi:10.1038/nrmicro1464

62. Fernandes P, Ferreira BS, Cabral JM. Solvent tolerance in bacteria: role of efflux pumps and cross-resistance with antibiotics. Int J Antimicrob Agents. Sep 2003;22(3):211-6. doi:10.1016/s0924-8579(03)00209-7

63. Bhakdi SM, N.; Menestrina, G. The hemolysin of Escherichia coli.

Eur J Epidemiol. 1988;4:135-143. doi:10.1007/BF00144740

64. Gilson L, Mahanty HK, Kolter R. Genetic analysis of an MDR-like export system: the secretion of colicin V. EMBO J. Dec 1990;9(12):3875-84. doi:10.1002/j.1460-2075.1990.tb07606.x

65. Ma D, Cook DN, Alberti M, Pon NG, Nikaido H, Hearst JE. Genes acrA and acrB encode a stress-induced efflux system of Escherichia coli. Mol Microbiol. Apr 1995;16(1):45-55. doi:10.1111/j.1365-2958.1995.tb02390.x

66. Abdallah J, Caldas T, Kthiri F, Kern R, Richarme G. YhbO protects cells against multiple stresses. J Bacteriol. Dec 2007;189(24):9140-4. doi:10.1128/JB.01208-07

67. Abdallah J, Mihoub M, Gautier V, Richarme G. The DJ-1 superfamily members YhbO and YajL from Escherichia coli repair proteins from glycation by methylglyoxal and glyoxal. Biochem Biophys Res Commun. Feb 5 2016;470(2):282-286. doi:10.1016/j.bbrc.2016.01.068

68. Osterman IA, Evfratov SA, Dzama MM, et al. A bacterial homolog YciH of eukaryotic translation initiation factor eIF1 regulates stress-related gene expression and is unlikely to be involved in translation initiation fidelity. RNA Biol. 2015;12(9):966-71. doi:10.1080/15476286.2015.1069464

ABSTRACT (IN KOREAN)

염증성장질환에서의 박테리아-박테리오파지 상호 작용의 이해

<지도교수 윤상선>

연세대학교 대학원 의과학과

용지현

염증성장질환에서의 박테리아-박테리오파지 간의 상호 작용의 이해를 위해 실험용 쥐의 장내에서 분리된 대장균 2주와 이들을 감염 및 용균할 수 있는 박테리오파지 두 종을 기반으로 한 모델 시스템을 구축하였다. 본 연구에서는 이 모델 시스템을 통하여 고농도의 활성산소가 존재할 때에, 장내 분리 대장균주들이 박테리오파지에 높은 저항성을 띄는 것을 확인하였다. 이러한 활성산소로 야기되는 파지 저항성에 관여하는 유전자의 동정을 위해 트랜스포손 시퀀싱 (Tn-sequencing) 을 활용하였다. 그 결과, 다중약물 유출펌프 (*mdtE*), 콜란산 캡슐 생합성 (*manC*), 독소 (*hokA*), 프로파지 절제효소 (*xisR*), 그리고 스트레스 반응과 관련된 유전자 (*yciH*, *yhbO*) 가

확인되었다. 염증성장질환에서는 활성산소의 농도가 건강한 사람의 장내에서 보다 높아져 있다는 점과, 동시에 장내 대장균이 늘어나 있으며, 그런 대장균을 포식하는 박테리오파지가 존재한다는 점을 보았을 때, 본 연구는 활성산소로 인한 대장균의 높아진 장내 박테리오파지 저항성이 염증성장질환에서의 잘 알려진 불균형한 대장균의 증식에 관여하는 요인 중 하나일 가능성을 제시한다.

핵심되는 말 : 대장균, 장내 공생균, 염증성장질환, 박테리오파지, 활성산소